Diffractive Pupil Telescope for high-precision space astrometry *(and coronagraphy!)*

Olivier Guyon (UofA)

Michael Shao (NASA JPL)	Improvements to original concept, error budget, exoplanet science
Stuart Shaklan (NASA JPL)	Error budget, mission architecture
Robert Woodruff (LMC)	Optical design for wide field telescope compatible with coronagraphy
Bijan Nemati (NASA JPL)	Numerical simulations, modeling approach
Mark Ammons (UofA)	Lab demo design & operation
Eduardo Bendek (UofA)	Lab demo optical design & operation
Marie Levine (NASA JPL)	System engineering, mission architecture
Joe Pitman (Expl. Sci.)	System engineering
Tom Milster (UofA)	Mask manufacturing, scaling of mask manufacturing to full scale PM
Jim Burge (UofA)	Mask manufacturing, scaling of mask manufacturing to full scale PM
Neville Woolf (UofA)	Exoplanet science, concept definition
Roger Angel (UofA)	Exoplanet science, concept definition
Josh Eisner (UofA)	Exoplanet and star formation/evolution science
Ruslan Belikov (NASA Ames)	Compatibility with coronagraphy
Daniel Eisenstein (UofA)	Extragalactic science enabled with wide field camera
Ann Zabludoff (UofA)	Extragalactic science with wide field camera
Dennis Zaritsky (UofA)	Extragalactic & galactic science with wide field camera
Jay Daniel (L3/Tinsley)	Optics manufacturing

Astrometry, Coronagraphy and exoplanets

Astrometry
Measures position of target star on sky
→ planet detection
→ planet mass, orbit

Implementation challenges:
Laser metrology, interferometry (Space Interferometry Mission)

Coronagraphy
Direct imaging of exoplanets and disk
→ planet detection
→ orbit
→ atmosphere composition → life finding

Implementation challenges:
Wavefront control and stability, pointing, chromaticity

Principle: use background stars around coronagraph target as an astrometric reference

With a 1.4-m telescope in the visible, 0.25 sq deg offers sufficient photons from stars at the galactic pole to provide an astrometric reference at the <50 nano-arcsec after taking into account realistic efficiency, zodi light and pixel sampling.

Why is imaging astrometry difficult ?

On-axis and off-axis stars illuminate different (but overlapping) parts of M2.
Edge bending on M2 is seen by star #1, but not star #2.

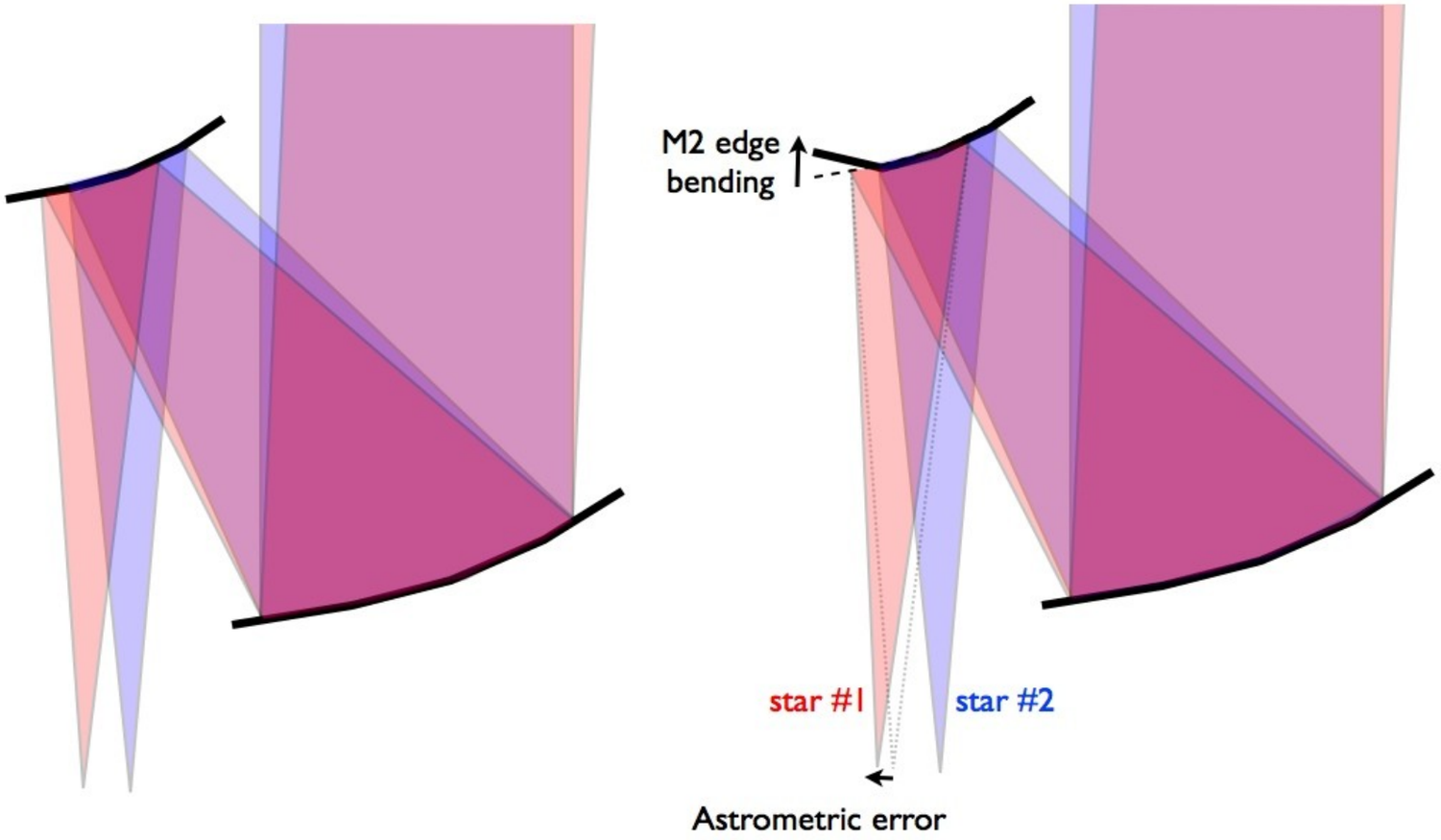

(1) Light from different stars on the sky travels different paths → small bending of optics produces field distortions

(2) The detector can move between observations (especially when using large mosaics)

(3) Pixels are not perfect and their response changes with time

+ (4) Central star is much brighter than background stars

Optical Layout for simultaneous coronagraphy and astrometry

The telescope is a conventional TMA, providing a high quality diffraction-limited PSF over a 0.5 x 0.5 deg field with no refractive corrector. The design shown here was made for a 1.4m telescope (PECO).
Light is simultaneously collected by the coronagraph instrument (direct imaging and spectroscopy of exoplanet) and the wide field astrometric camera (detection and mass measurement of exoplanets)

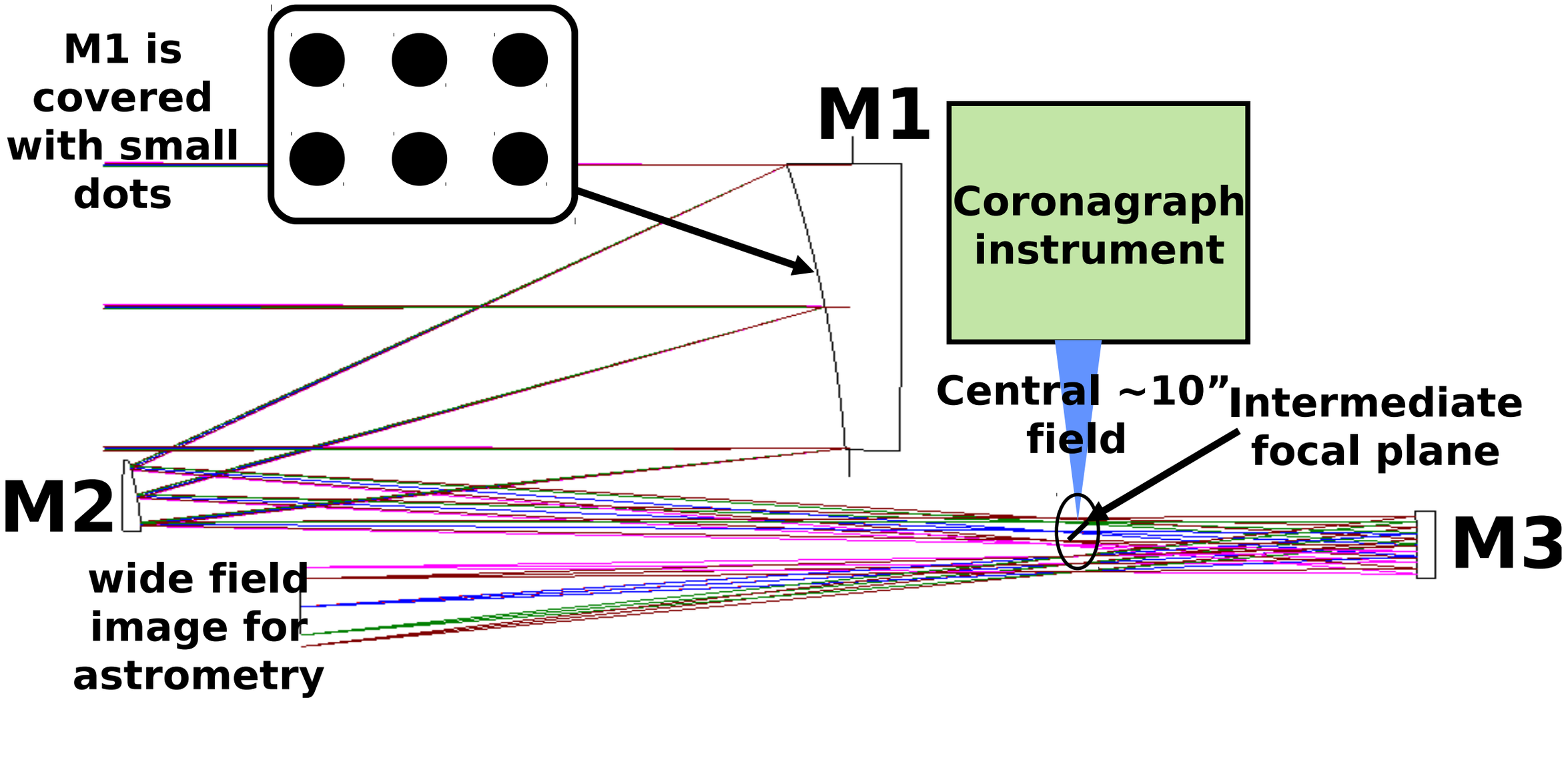

Dots on primary mirror create a series of diffraction spikes used to calibrate astrometric distortions

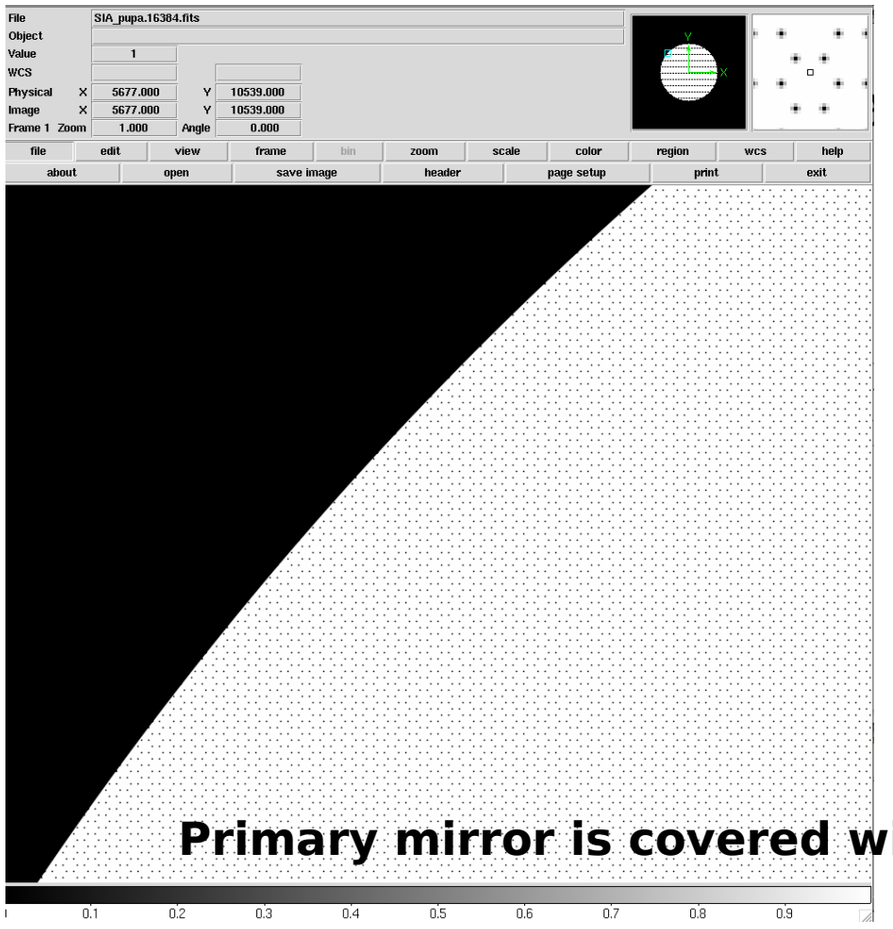

Primary mirror is covered with small dots

The center of the field is missing from the astrometric camera (central light is sent to coronagraph)

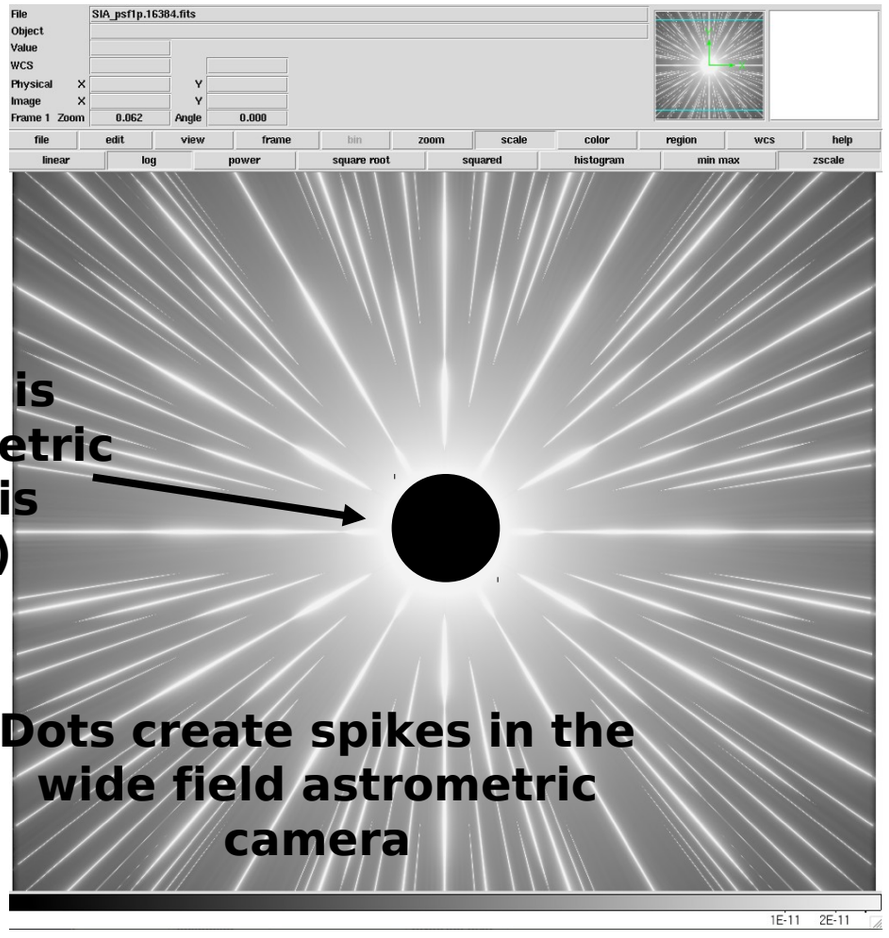

Dots create spikes in the wide field astrometric camera

All astrometric distortions (due to change in optics shapes of M2, M3, and deformations of the focal plane array) **are common to the spikes and the background stars**. By referencing the background star positions to the spikes, the astrometric measurement is largely immune to large scale astrometric distortions.
Instead of requiring ~pm level stability on the optics over yrs, the stability requirement on M2, M3 is now at the nm-level over approximately a day on the optics surfaces, which is within expected stability of a coronagraphic space telescope. (Note: the concept does not require stability of the primary mirror).

Precursors...

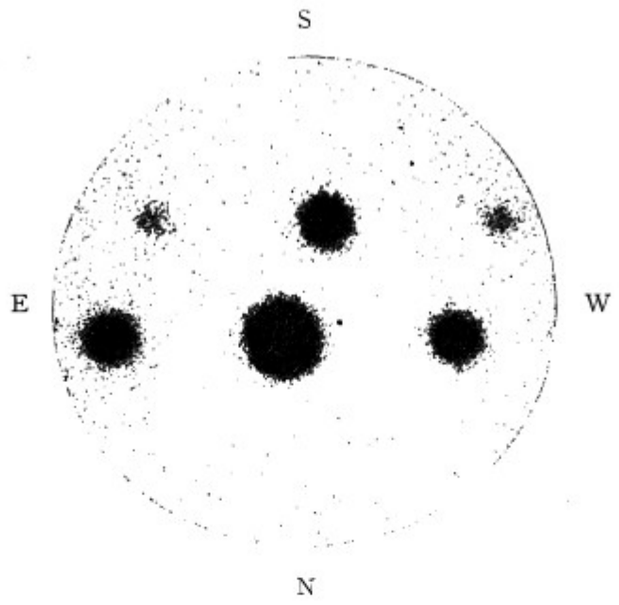

A 5-seconds exposure of Castor, enlarged 75 times. The separation of the components is 3".74 or 0.198 mm on the plate. The first order spectra are one magnitude fainter than the central image. Taken December 1, 1939, by K. Aa. Strand, with the Sproul 24-inch refractor, aperture reduced to 13 inches, Eastman IV G emulsion, Wratten No. 12 (minus-blue) filter.

age of the fainter component, a compensation for possible magnitude error is provided by using the mean of the measured positions of the two spectral images instead of the central image. As long as the difference in intensity between the images does not exceed half a magnitude, the magnitude error is usually negligible; it is therefore sufficient to have a limited number of gratings, producing first-order spectra which are a whole number of magnitudes fainter than the central image. For example, in his work with the Sproul refractor, Strand[8] used four gratings, made of duraluminum, giving differences of one, two, three, and four magnitudes, respectively, between the central image and the first-order spectra. The bars are mounted on 10 cm-wide annular frames, cut from sheets of duraluminum, 3 mm thick. The constants of the four gratings are given below.

CONSTANTS OF SPROUL OBJECTIVE GRATINGS

Grating	——width of—— bar	opening	extinction for central image	first order minus central image mag. difference	distance
1	11.25 mm	11.21 mm	1.51 mag	.98 mag	.270 mm = 5".10
2	7.12 mm	15.06 mm	.84 mag	2.05 mag	.273 mm = 5.15
3	3.98 mm	14.80 mm	.52 mag	3.01 mag	.322 mm = 6.08
4	3.20 mm	19.06 mm	.34 mag	3.95 mag	.272 mm = 5.13

"Long-focus photographic astrometry", van de Kamp, 1951

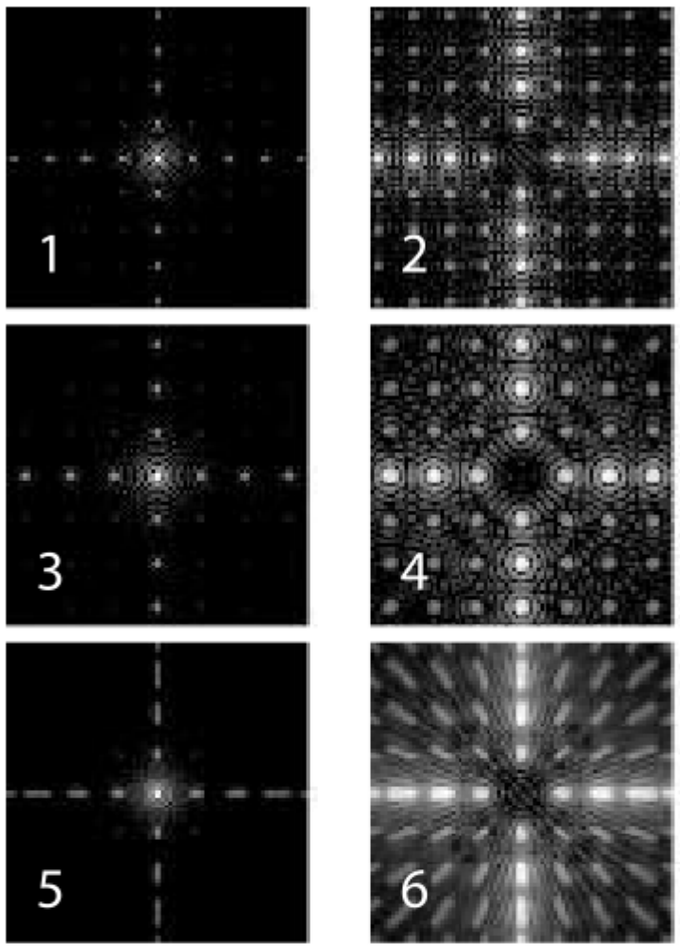

FIG. 1.—Monochromatic and broadband direct and coronagraphic PSFs with a square-geometry reticulate pupil mask. All images are on a logarithmic gray scale stretching 10 mag fainter than their peaks. The pupil is 128 pixels across, and the grid has a wire spacing of 16 pixels, with 2-pixel-wide wires. (1): Direct PSF for the shortest wavelength of a 20% bandwidth filter with uniform transmission within the bandpass, in the absence of phase errors. The satellite PSFs off the origin but along the horizontal and vertical axes are fainter than the central core of the PSF by a factor $\epsilon^2 = (g/d)^2$, where g is the wire thickness and d is the wire spacing. The satellite spots off the axes are ϵ^4 fainter than the corresponding central peak. (2): Coronagraphic PSF at the shortest wavelength of the filter. The off-axis sea of satellite spots are more visible in the coronagraphic image because the core has been suppressed. (3) and (4): Direct and coronagraphic PSFs for the longest wavelength of the filter. (5) and (6): Direct and coronagraphic PSF for the full bandpass. The length of any particular radial streak in this last pair of images (in resolution elements at the central wavelength of the bandpass) is approximately the fractional filter bandwidth multiplied by the radial distance of the spot at band center. The streaks all point toward the origin, so the smearing has no effect on astrometric precision according to Fraunhofer regime image formation theory. We suggest using the four satellite peaks closest to the core as fiducials for the position of the central occulted star in coronagraphic images.

"Astrometry and Photometry with Coronagraphs", Sivaramakrishnan, Anand; Oppenheimer, Ben R., 2006

Red points show the position of background stars at epoch #1 (first observation)

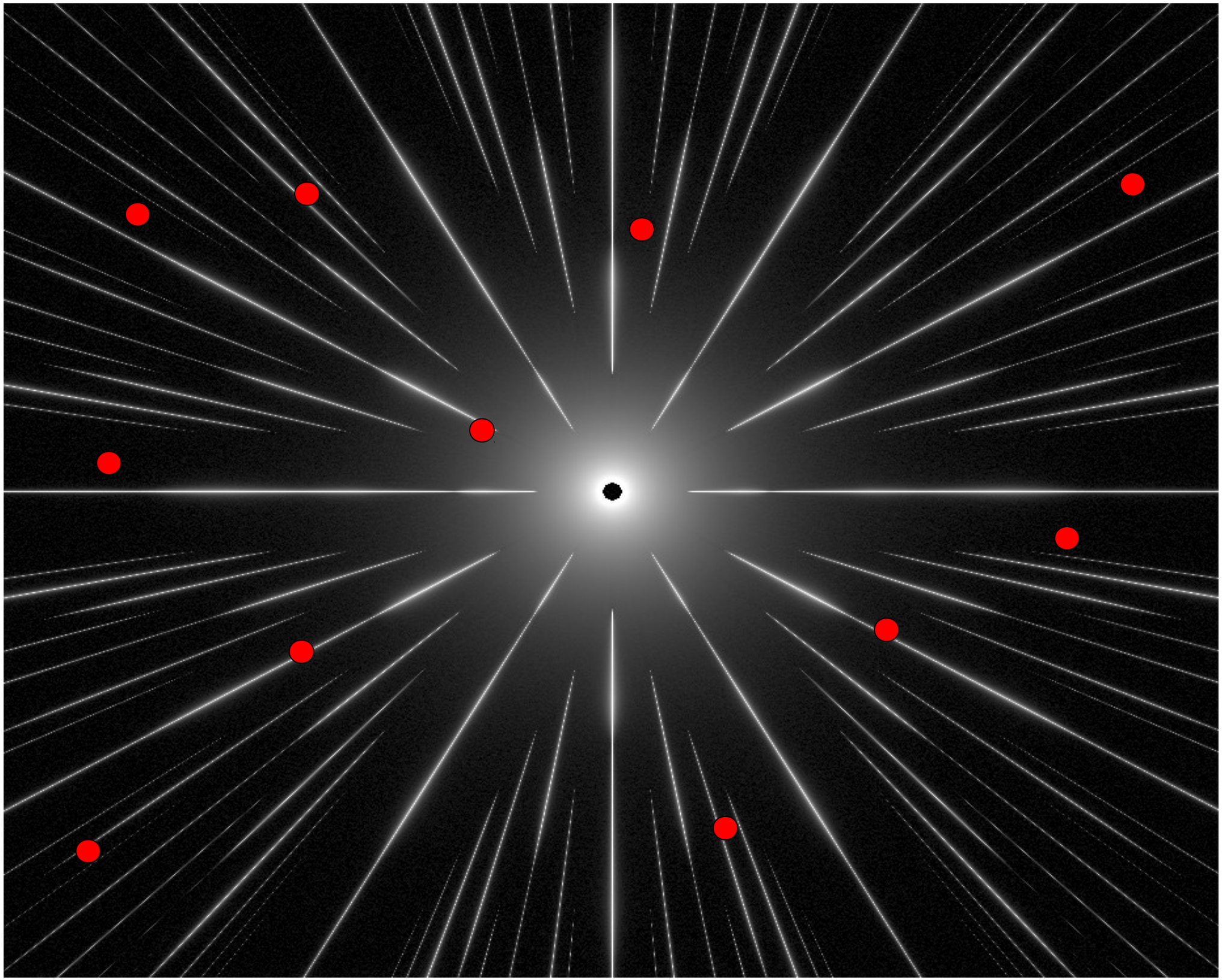

Blue points show the position of background stars at epoch #2 (second observation) The telescope is pointed on the central star, so the spikes have not moved between the 2 observations, but the position of the background stars has moved due to the astrometric motion of the central star (green vectors).

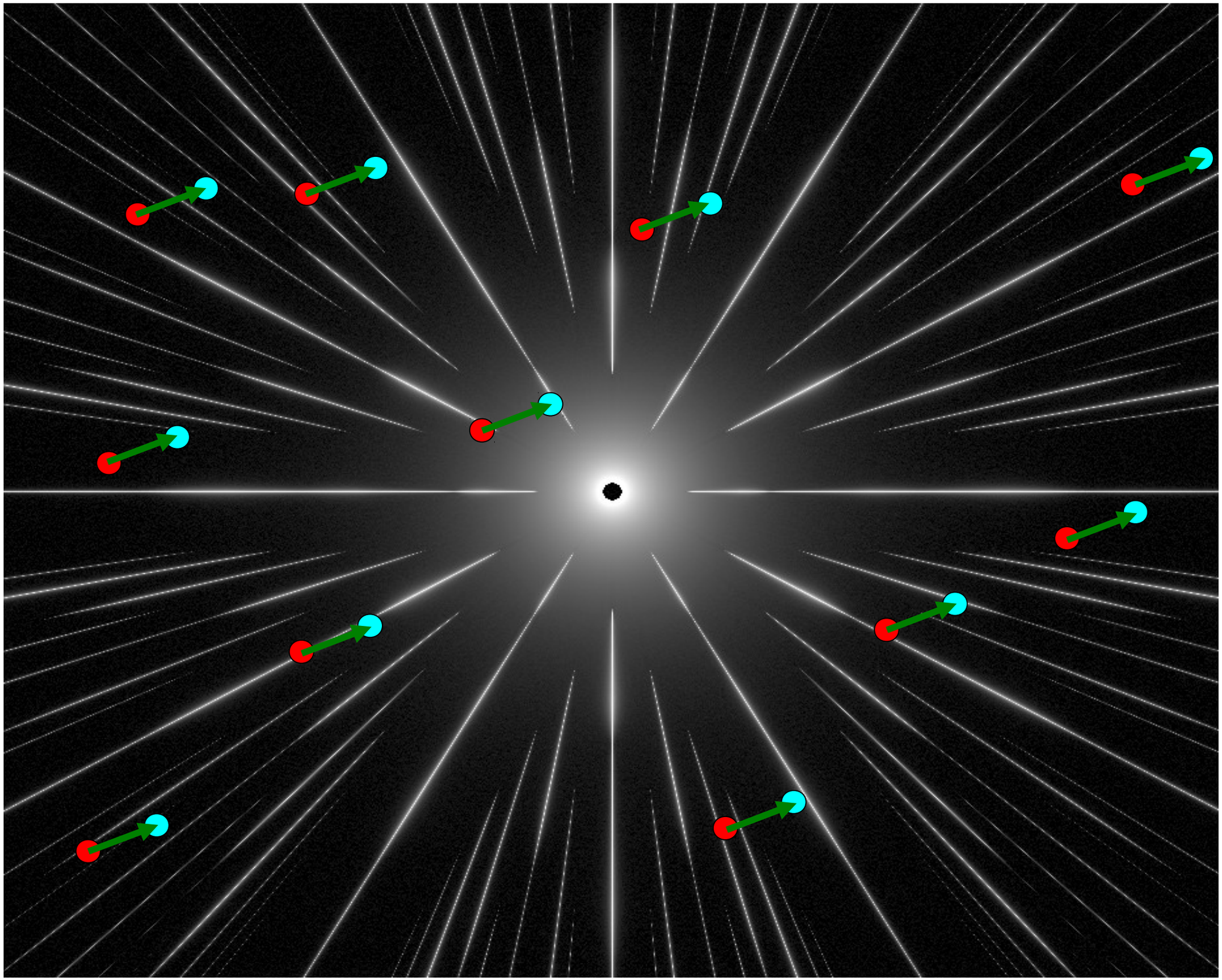

Due to astrometic distortions between the 2 observations, the actual positions measured (yellow) are different from the blue point. The error is larger than the signal induced by a planet, which makes the astrometric measurement impossible without distortion calibration.

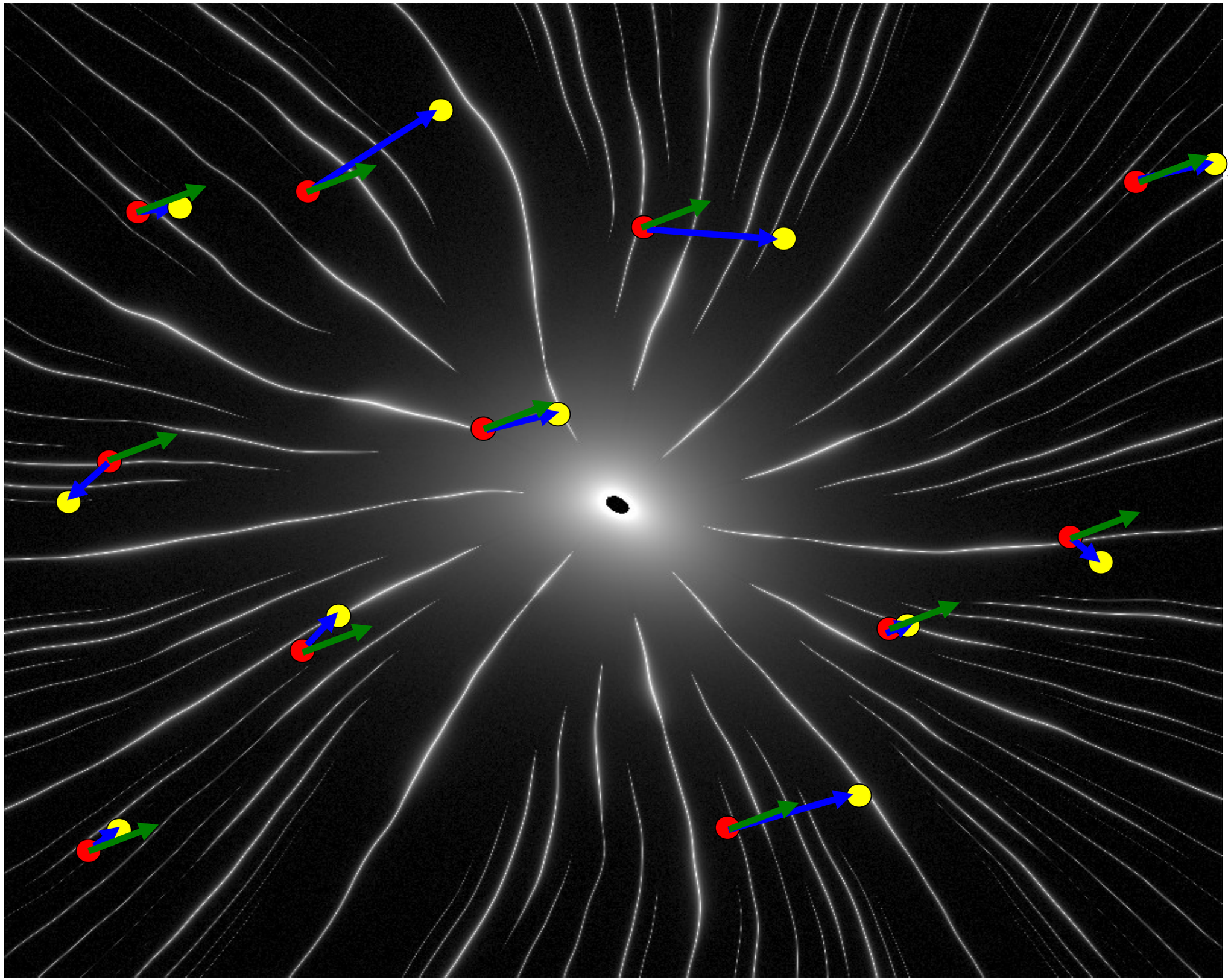

The measured astrometric motion (blue vectors in previous slide) is the sum of the true astrometric signal (green vectors) and the astrometric distortion induced by change in optics and detector between the 2 observations.
Direct comparison of the spike images between the 2 epochs is used to measure this distortion, which is then subtracted from the measurement to produce a calibrated astrometric measurement.

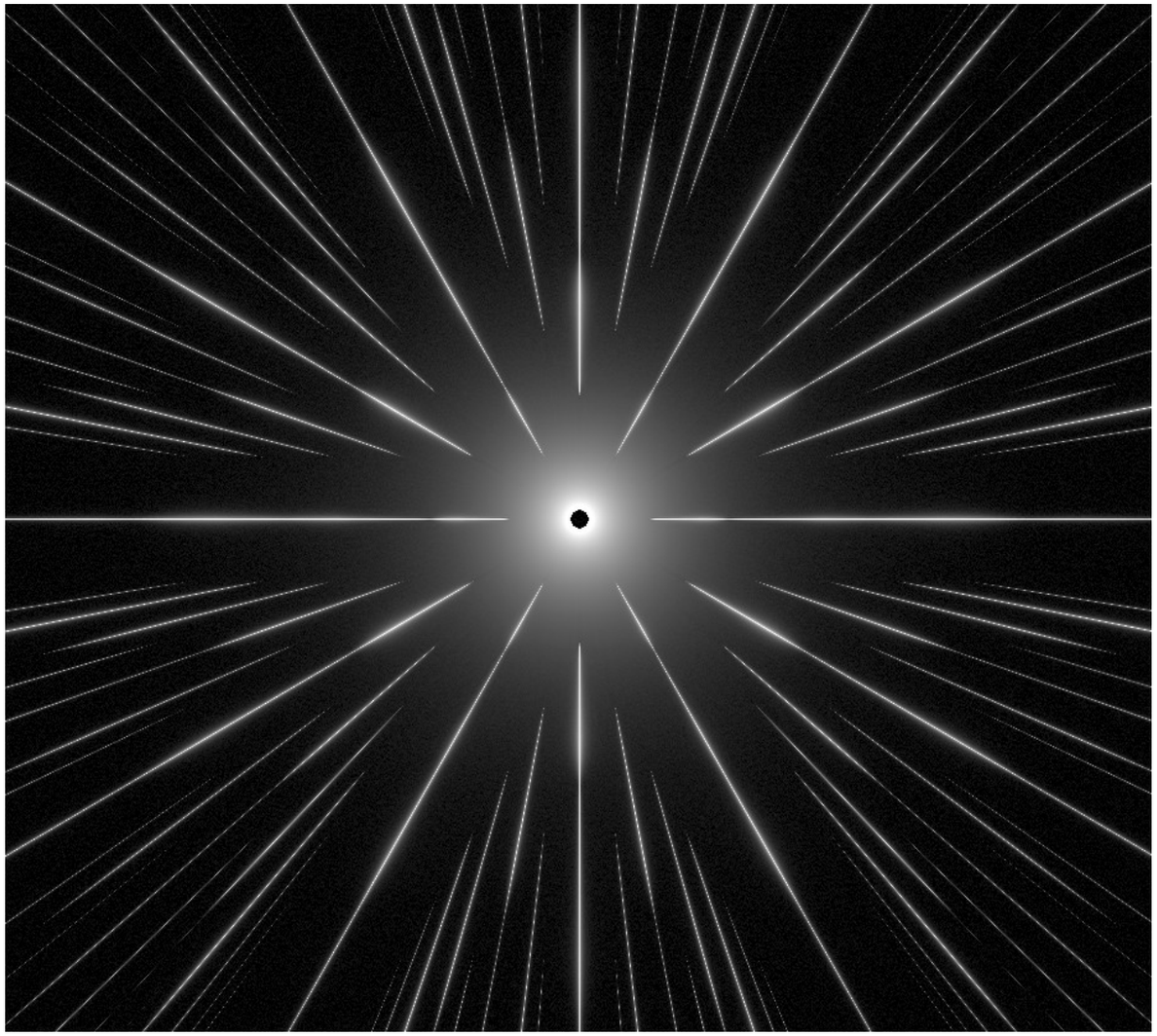

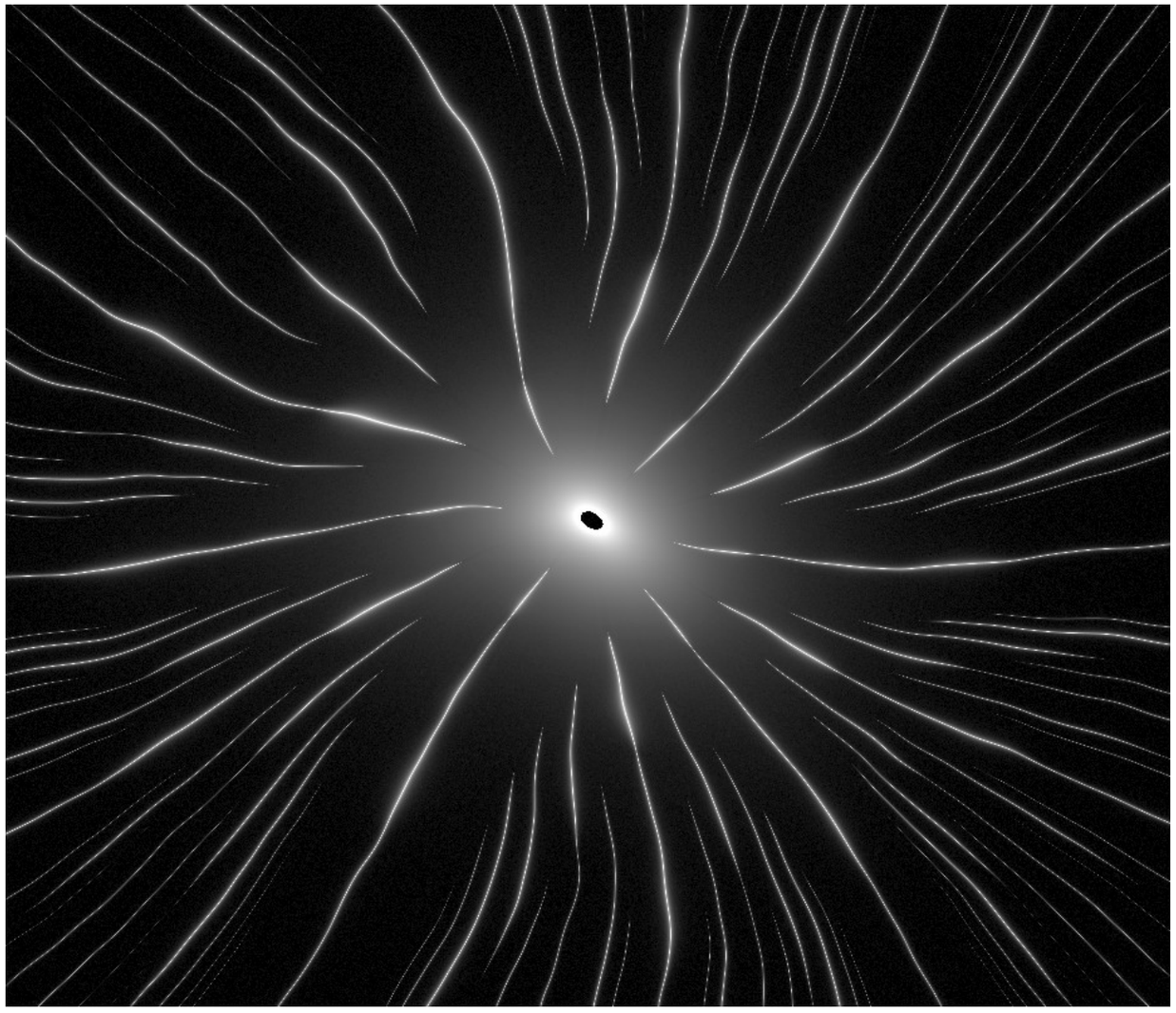

The calibration of astrometric distortions with the spikes is only accurate in the direction perpendicular to the spikes length. For a single background star, the measurement is made along this axis (1-D measurement), as shown by the green vectors. The 2-D measurement is obtained by combining all 1-D measurements (large green vector).

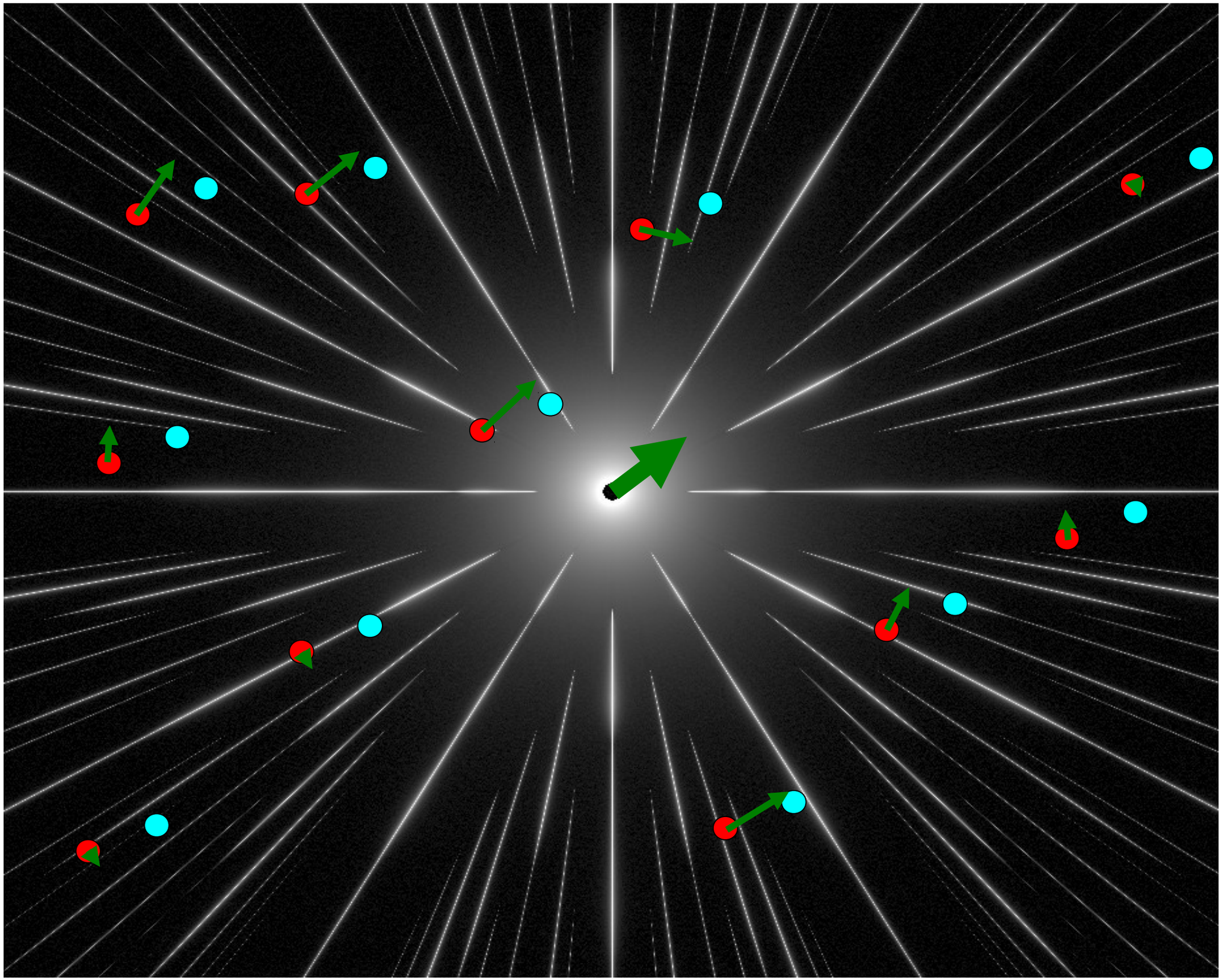

Observation scheme

A slow telescope roll is used to average out small scale distortions, which are due to non-uniformity in the pixel size, (spectral) response, and geometry

The green vector is what should be measured

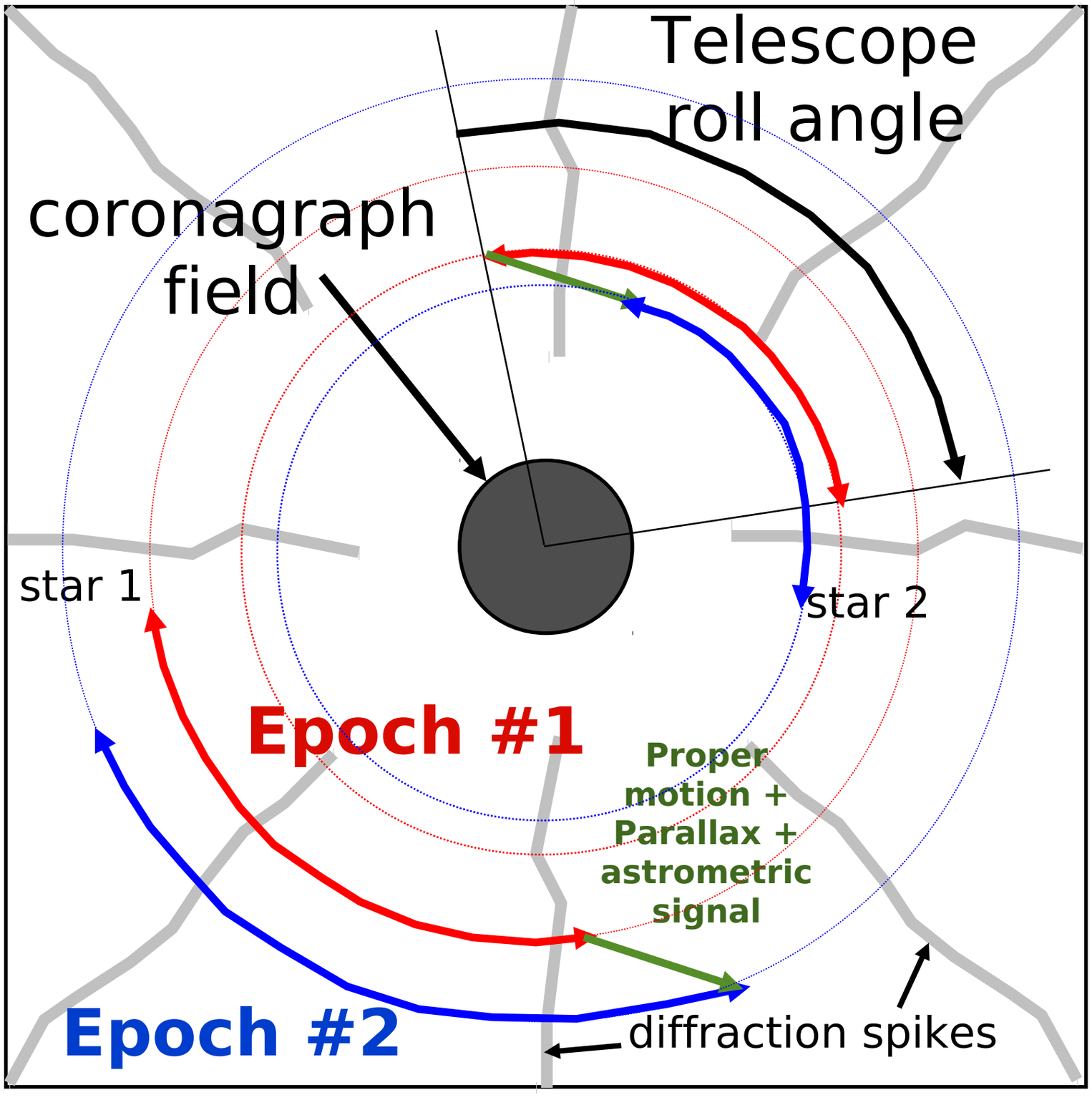

Science goals

Primary science goal:

Measure planet mass with 10% accuracy (1-σ) for an Sun/Earth analog at 6pc.

This allows mass measurement of all potentially habitable planets (Earth-like & SuperEarths) imaged by PECO.

SNR>5 detection at R=5 in less than 6 hrs along 20% of the planet orbit, assuming 45% system efficiency, and 1 zodi (no WF errors)

Table 4-2: Stars with Earth-like planets in habitable zones (1 AU equiv) easily detectable with PECO

HIP#	dist (pc)	max el (λ/D)	*rad (λ/D)	SNR (1s, tp)	t20% (s, tp)	Comment
71683	1.3	11.5	0.06	0.49	35	Alf Cen A G2 V, V=0
71681	1.3	6.6	0.04	0.45	44	Alf Cen B K2 IV, V=1.3
8102	3.6	2.3	0.01	0.08	2750	Tau Cet G8.5 V, V=3.5 **
16537	3.2	2.2	0.01	0.09	2968	Eps Eri K2 V, V=3.7 **
3821	6.0	2.3	0.01	0.04	14329	Eta Cas G0 V V=3.5 ***
2021	7.5	3.1	0.01	0.03	14878	Bet Hyi G0 V, V=2.8
99240	6.1	2.2	0.01	0.03	19636	Del Pav G8 IV, V=3.6

Table extracted from PECO SRD (http://caao.as.arizona.edu/PECO/PECO_SRD.pdf)

Simulated observations

Planetary system characteristics	
Star	Sun analog
Distance	6 pc
Location	Ecliptic pole
Orbit semi-major axis	1.2 AU
Planet mass	1 Earth mass
Orbit excentricity	0.2
Astrometric signal amplitude	0.5 µas
Orbit apparent semi-major axis	200 mas
Observations	
Number of observations	32 (regularly spaced every 57 days)
Coronagraph: planet position measurement accuracy in coronagraphic image	2.5 mas per axis (= 3.6 mas in 2D): corresponds to diffraction-limited measurement with 100 photon at 550 nm on PECO
Coronagraph: Inner Working Angle	130 mas (coronagraph cannot see planet inside IWA)
Astrometry: accuracy	Variable (to be matched to science requirements)

Combined solution derived from simultaneous coronagraphy and astrometry measurements

Known variables:

- **Star location** on the sky (effect of parallax is known except for star distance, aberration of light perfectly known)
- **observing epochs**
- **Stellar mass** (assumed to be known at the 5% accuracy level)
- **measurement noise levels** for astrometry (~μas), coronagraphy planet position (few mas) and star mass (~5%)

Measurements

Astrometry:
star position
(nb of variables =
2x #observations)

Coronagraphy:
planet position
(nb of variables =
2x #observations)

Solution

Maximum likelihood solution for
11 free parameters to be solved for:

- star parallax (1 variable)
- proper motion (2 variables)
- star mass (1 variable)
- planet mass (1 variable)
- orbital parameters (6 variables)

Combined solution for simultaneous coronagraphy + astrometry

Planet on a 1.2 AU orbit (1.3 yr period), e=0.2
orbit orientation on sky: planet outside the coronagraph IWA for 17 out of the 32 observations.

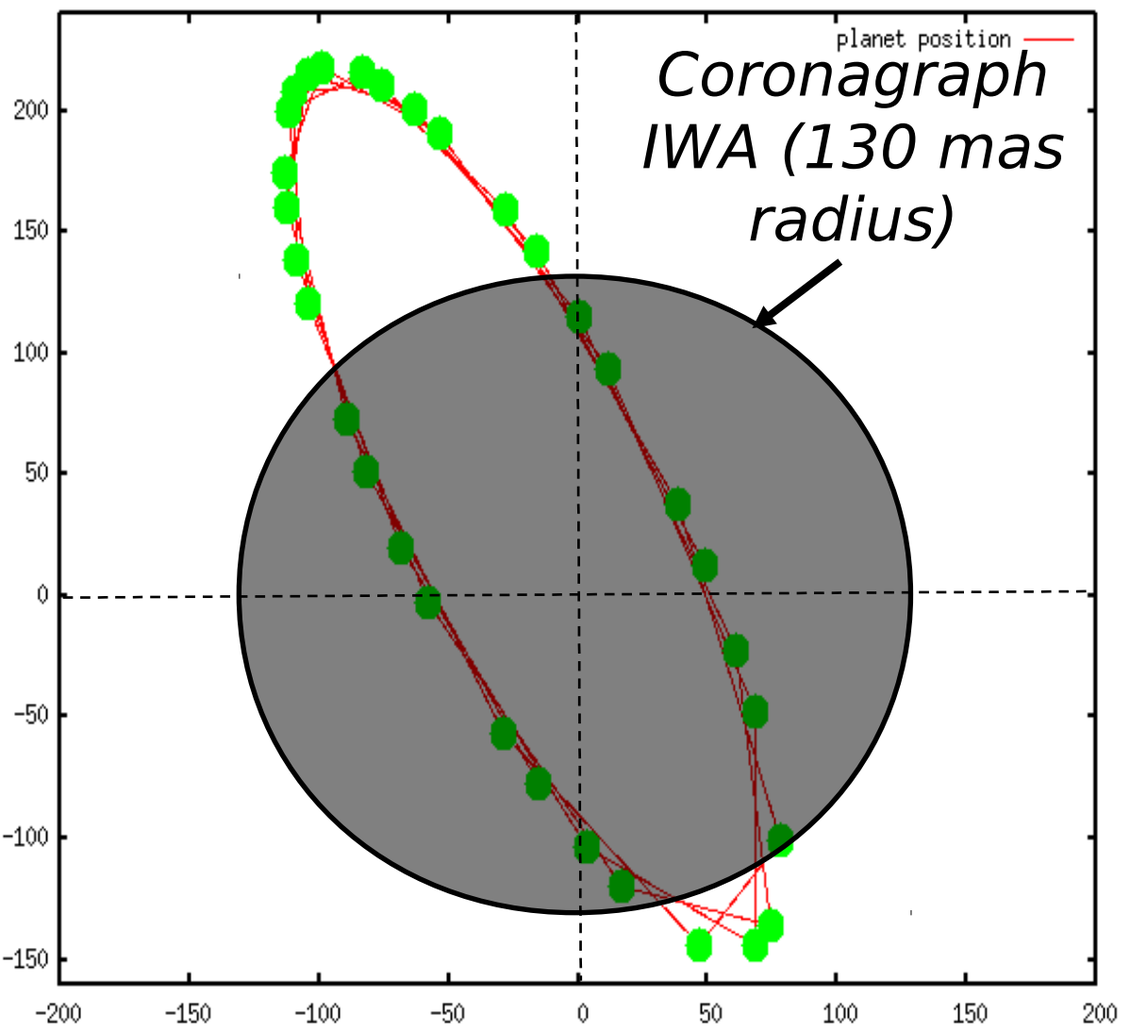

Required single measurement astrometric accuracy = 0.2 μas (1-sigma, 1D)

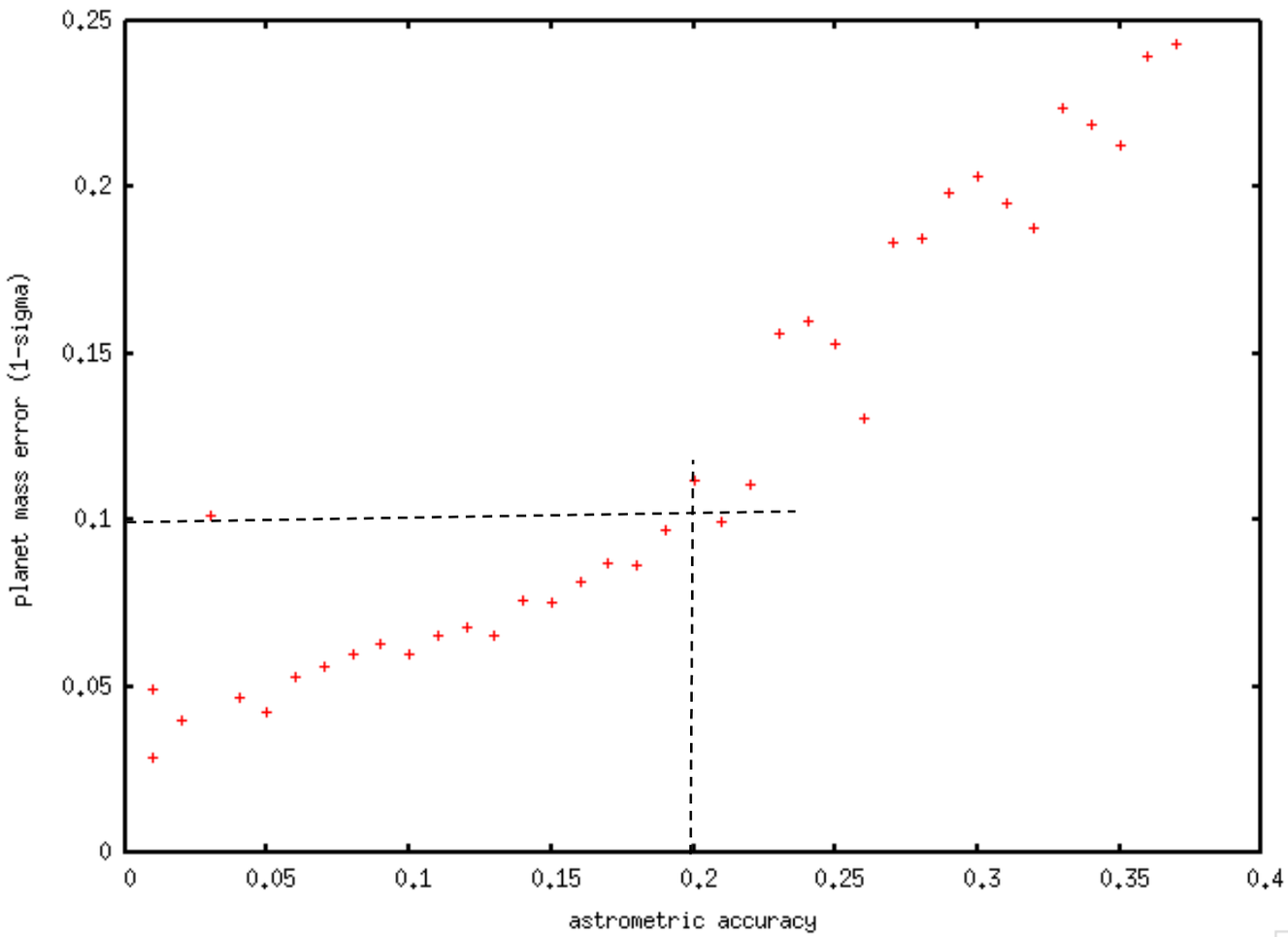

Combined solution for simultaneous coronagraphy + astrometry is very accurate for orbital parameters measurement

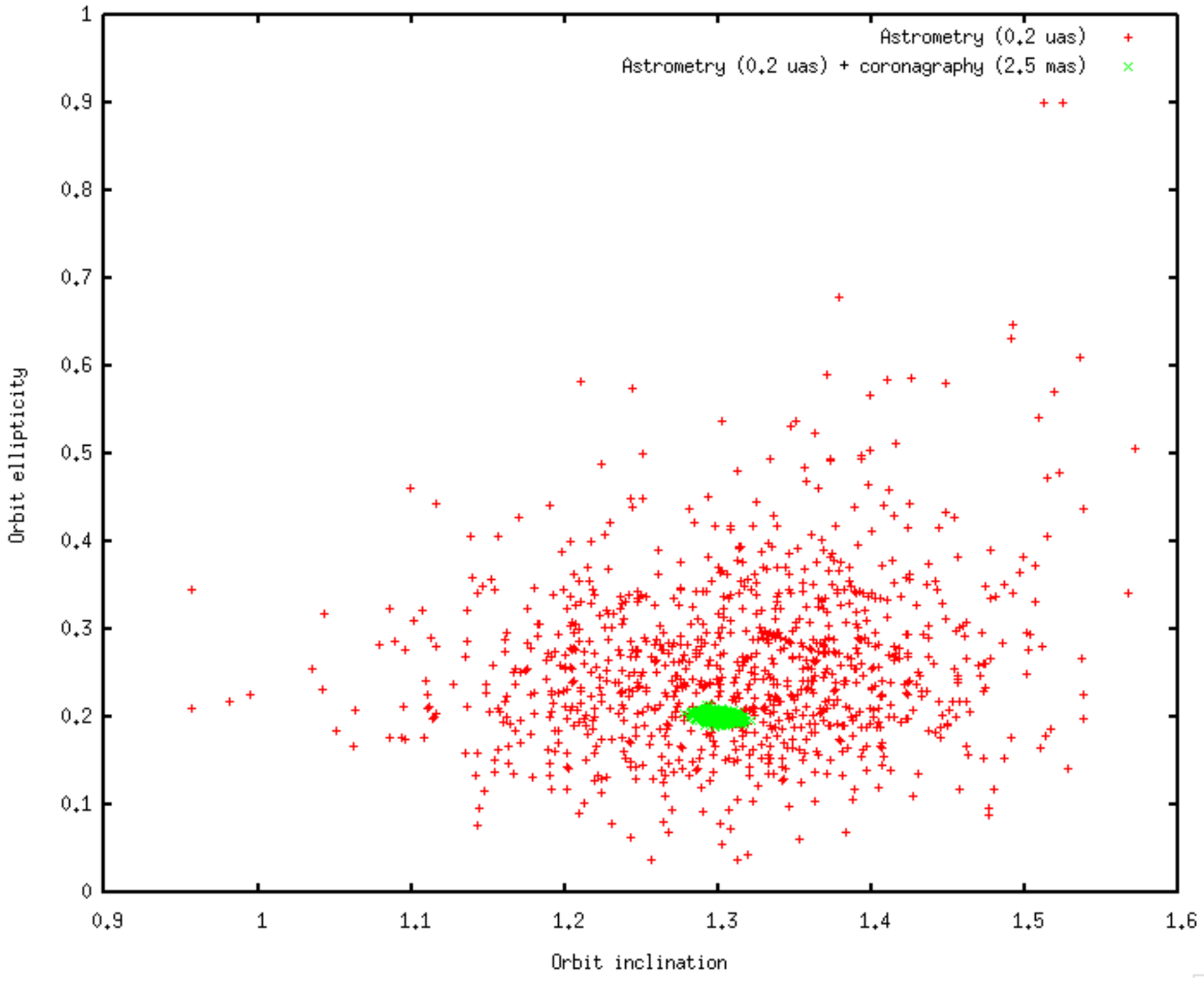

Better estimate of orbital parameters -> better planet mass estimate

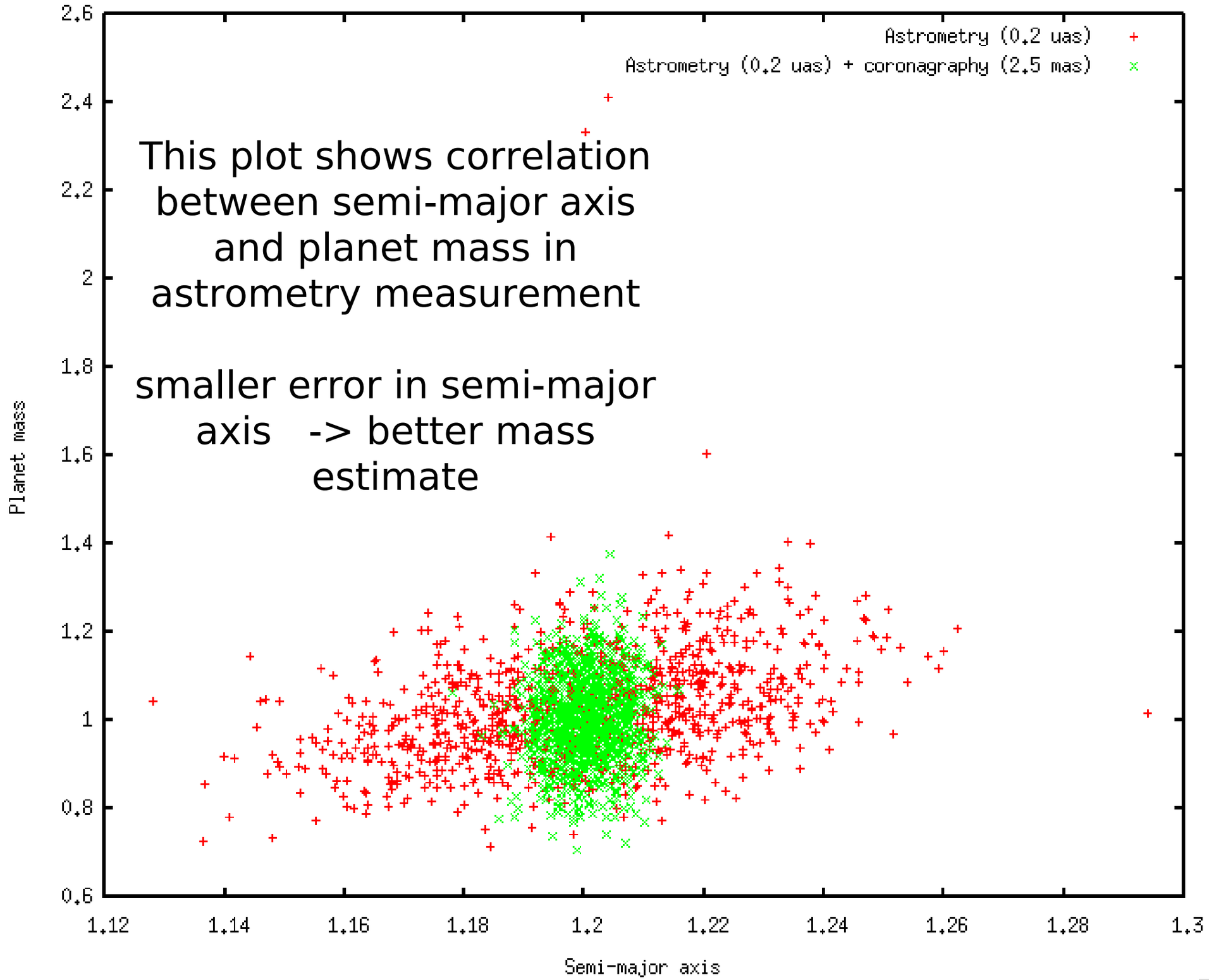

Better estimate of stellar mass -> better planet mass estimate

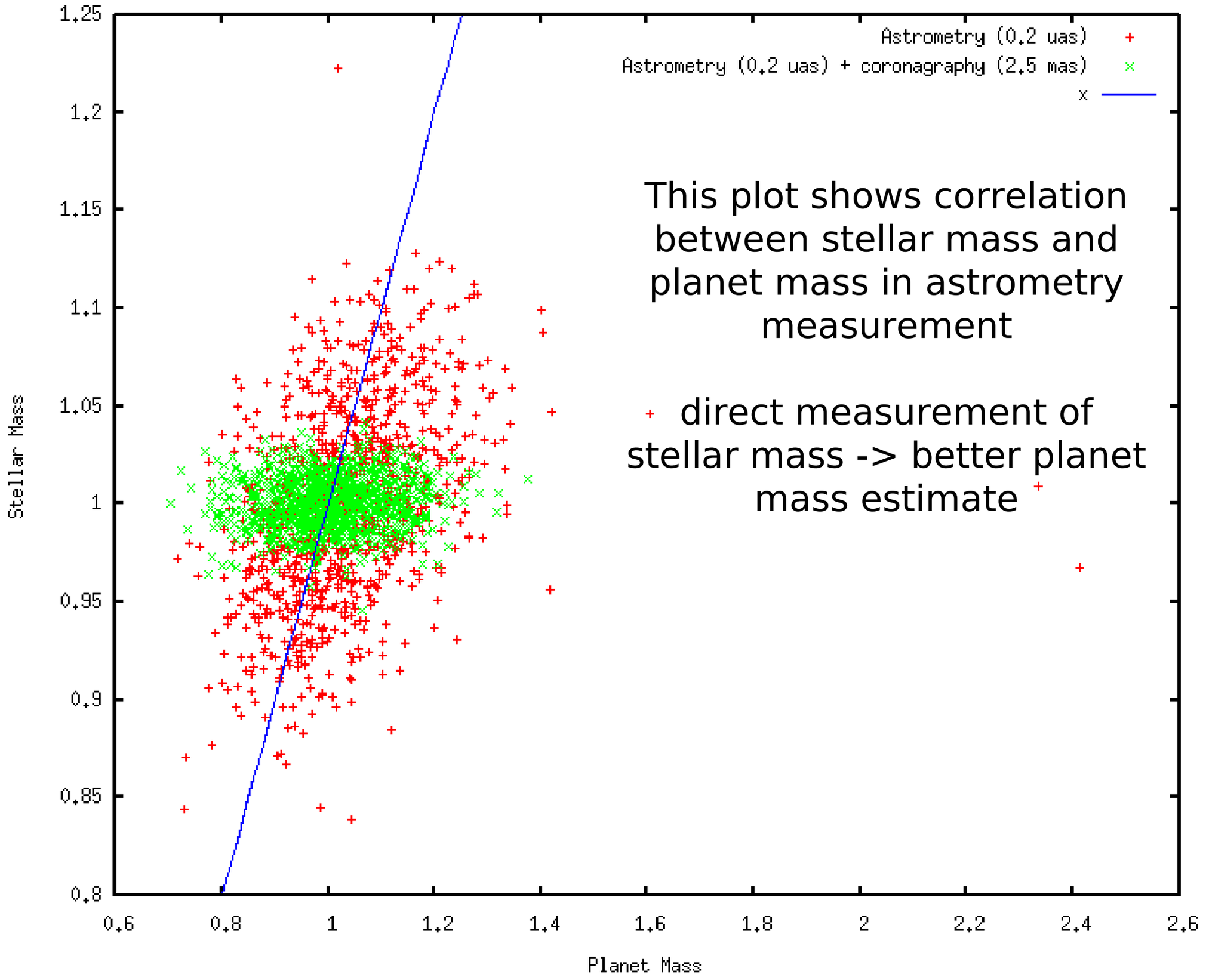

Combined solution for simultaneous coronagraphy + astrometry

	Standard deviation	
	Astrometry only	**Astrometry + coronagraphy**
parallax	0.037 μas	0.035 μas
x proper motion	0.017 μas/yr	0.012 μas/yr
y proper motion	0.020 μas/yr	0.013 μas/yr
Planet mass	0.132 ME	0.098 ME
Semi-major axis	0.0228 AU	0.0052 AU
orbital phase	0.653 rad	0.039 rad
orbit inclination	0.0968 rad	0.0065 rad
sma projected PA on sky	0.1110 rad	0.0040 rad
orbit ellipticity	0.098	0.0035
PA of perihelion on orbit plane (w)	0.648 rad	0.0034 rad
star mass	0.050 MS	0.013 MS

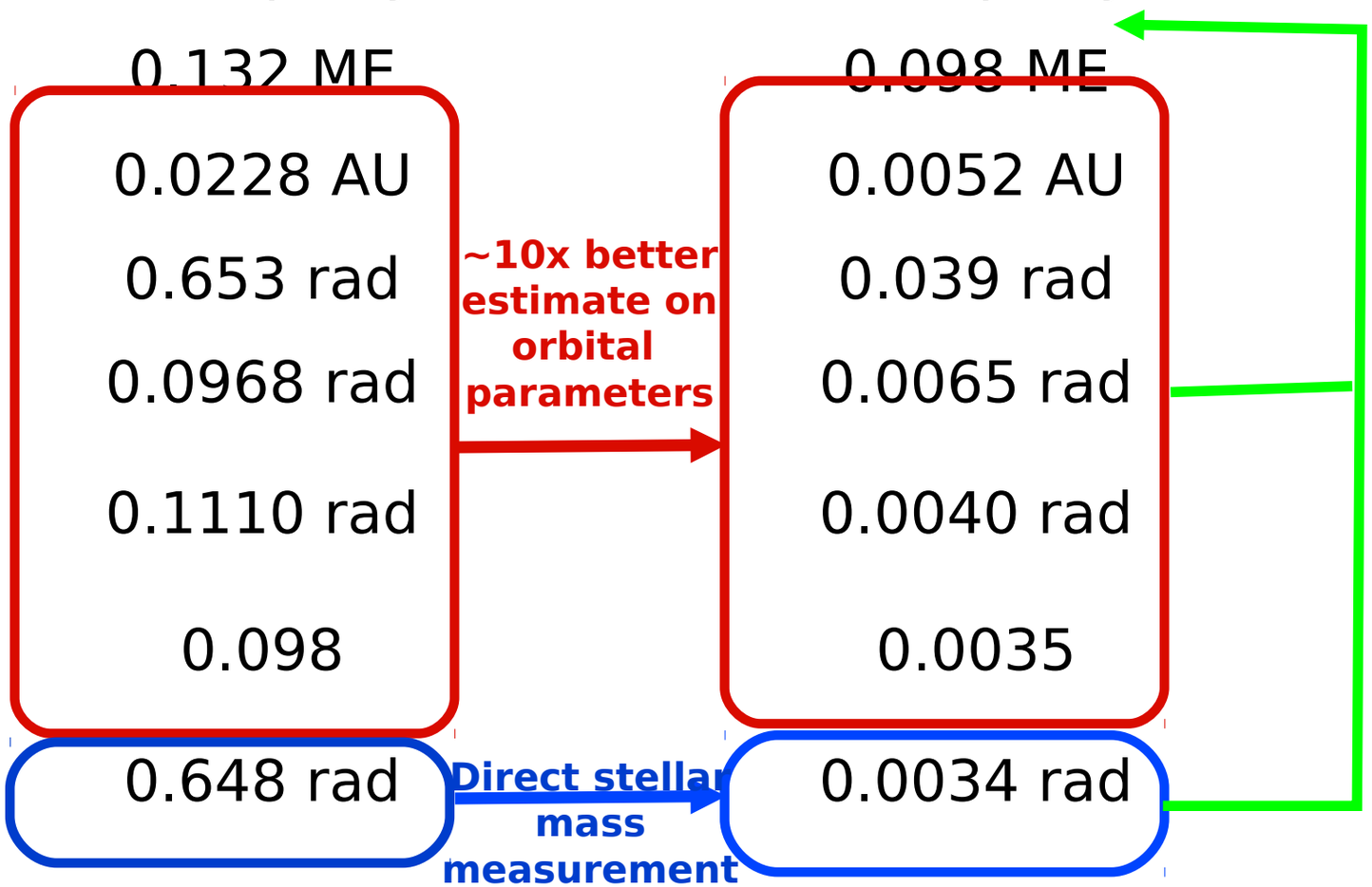

Benefits of simultaneous coronagraphy + astrometry

Solving for planet orbit and mass using the combined astrometry + coronagraphy measurements is scientifically very powerful:

- **Reduces confusion with multiple planets**. Outer massive planets (curve in the astrometric measurement) will be seen by the coronagraph.

- Astrometry will **separate planets from exozodi clumps**.

- Astrometric knowledge allows to **extract fainter planets from the images, especially close to IWA**, where the coronagraph detections are marginal.

- Mitigates the **1yr period problem** for astrometry

	Value in simulations	Value for mission	Rationale for flight instrument value	Impact on astrometric accuracy
Telescope diameter (D)	1.4 m		PECO sized, cost constrained	Astrometric accuracy goes as D^{-2}, thanks to larger collecting area and smaller PSF size (assuming constant FOV)
Detector pixel size	44 mas		Nyquist at 600 nm	Little impact as long as sampling is close to or finer than Nyquist
Field of view (FOV)	0.03 sq deg (0.1 deg radius)	0.25 sq deg (0.5 deg X 0.5 deg)	low WF error across field, 1.6 Gpix detector	Astrometric accuracy goes as $FOV^{-0.5}$
Single measurement time	48 hr		Typical single observation duration for coronagraph	Astrometric accuracy goes as $t^{-0.5}$
Dot coverage on PM (area)	1%	8%	Keeps thoughput loss moderate in coronagraph	Larger dot coverage allows observation of fainter sources.
Flat field error after calibration, static (high spatial frequency)	1.02% RMS, 6% peak		Conservative estimate for modern detector after calibration	Negligible effect on background PSF measurement (well averaged with roll)
Flat field error, dynamic	1e-4 RMS per pixel, uncorrelated spatially and temporally between observations		1e-4 loss in sensitivity for each pixel over 48 hrs = 2% per year = 10% over 5 yrs	Negligible effect on background PSF measurement, but significant effect on measurement of spikes locations
Telescope roll	1.0 rad (+/- 0.5 rad)		Manageable sunshielding	Larger telescope roll leads to better averaging of detector errors
Uncalibrated change in optics surface between observations for M2 & M3	40 pm		Wavefront measurement repeatability (optical element removed / reinserted) obtained when testing similar sized optics on ground	Larger change in optics surface reduces astrometric accuracy
Static optics surface errror (M3 mirror)	1.5 nm		WF error and PSD taken from similar existing optical element	Small impact on performance, as background PSFs are almost fixed between observations
Astrometric accuracy, single measurement, single axis, m_V=3.7, galactic pole	***0.58 µas***	***0.20 µas***	***0.2 µas is required to achieve science goals***	

Simulation description

Simulation details available on: www.naoj.org/staff/guyon/
(60 slides describing next chart)

Simulation assumes:

- 1.4m telescope TMA (Woodruff design)
- 1.5nm surface (3nm WF) optics for M2 and M3, PSD provided by Tinsley
- Circular field of view, 0.2 deg diam (0.03 sq deg)
- Galactic pole observation (worst case scenario)
- central star is m_v=3.7 (faintest of the 7 PECO targets for which an Earth can be imaged in <6hr, 14th brightest target in the 20 high priority targets list)
- 90% detector peak QE, 80% optical throughput (0.96^3 for optics reflectivity x 0.92 due to dots on PM)
- Nyquist sampled detector at 0.6 micron = 44 mas pixels
- Telescope roll = 1 rad (larger angle = better averaging, but more difficult to maintain stability)
- Single epoch observation = 2 day

Distortions in the system are computed with 3D raytracing (code written in C, agreement with Code V results from Woodruff has been checked)
Images produced by Fourier transform, and then distorted according to geometrical optics. Image sizes are 16k x 16k.

Numerical simulation approach

pupil mask with dots
pupa

Monochromatic PSF
psf1m

Polychromatic PSF
psf1p

PSF x derivative
PSF y derivative
psfpdx, psfpdy

PSF angular derivative
psfpdr

distortion measurement SNR per pixel for a 1 pixel angular distortion

square & bin

snrim

Dynamic distortions

focal plane array x and y distortion change
fpdistx, fpdisty

mirrors M2 and M3 surface change

raytracing

variation in detector flat field response
fferror

total x and y distortion change
distx, disty

distvarx, distvary

optics x and y distortion change
optdistx, optdisty

angular distortion change
distr

photon noise due to zodiacal background and stellar flux

measured spikes image
mpsf

signal
signal

binned square SNR per pixel for a 1 pixel angular distortion
snr2bin

SNR^2-weighted binning

binned angular distortion signal
signalbin

SNR-weighted convolution by anisoplanatism sized kernel

binned angular distortion measurement
mdistrbin

binned angular distortion change
distrbin

quick look at residual distortion (useful for optimizing anisoplanatism kernel)

bilinear interpolation

photon noise error due to zodiacal light and stellar flux

background star position measurement error (angular direction)

roll averaged residual distortion error map in angular direction
astrerrordyn

roll averaging

residual astrometric distortion error map in angular direction
resdist

measured astrometric distortion map in angular direction
mdistr

roll averaging

detector flat field error
ffsta

static angular distortion
distr_sta

background stars position measurement errors between 2 epochs (1-D angular coordinate)

optimal weighting of all 1-D measurements

2-D astrometric measurement

Static distortions

focal plane array x and y distortion
fpdistx_sta, fpdisty_sta

mirrors M2 and M3 surface errors

raytracing

total x and y distortion
distx_sta, disty_sta

optics x and y distortion
optdistx_sta, optdisty_sta

Sum of two or more images

Difference between two images

Product of two images (pixel by pixel)

Image name (used through this document)

Operation performed on images or data

single star photon noise limited error
photon noise limit, monochromatic PSF, infinite sampling, no background
actual measurement error
measurement error (1-sigma)

shorter observation time

longer observation time

zodi background

finite detector sampling, polychromatic PSF

accuracy floor due to distortions & detector limits

shorter detector readout

Detector saturation

poor detector calibration
unstable optical system and focal plane array

stable optical system and focal plane array

good detector calibration

1.4m telescope
0.1 deg field radius
(0.03 sq deg)
galactic pole
2 day observation

1-D astrometric accuracy, 1 sigma (arcsec)

0.01
0.001
0.0001
1e-05
1e-06
1e-07
1e-08

12
14
16
18
20
22
24
26
28
30

Star brightness (mV)

Performance as a function of star brightness (FOV = 0.03 sq deg)

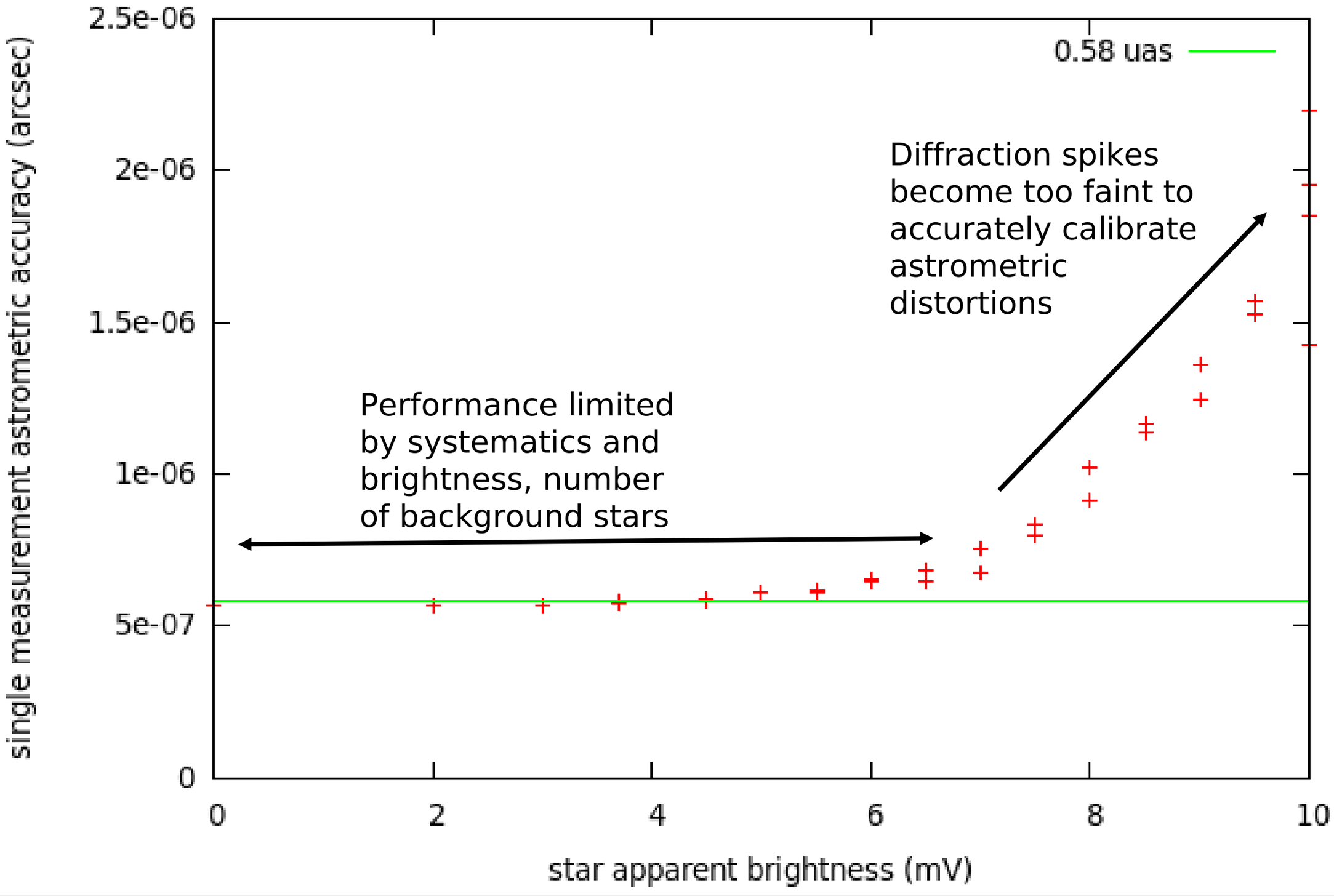

Astrometry + coronagraphy can precisely measure mass and orbital parameters of multiple planets systems

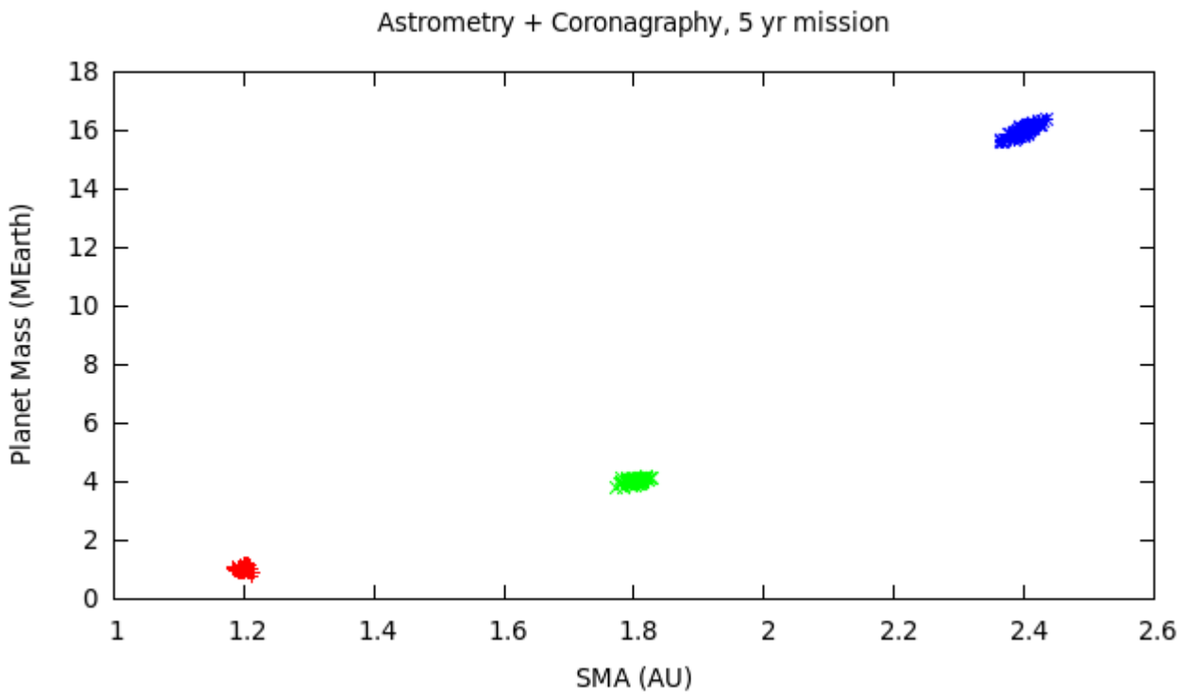

Astrometry+Coronagraphy,
Coronagraphy only :
1 observation every 2 month

Astrometry only:
1 observation per month

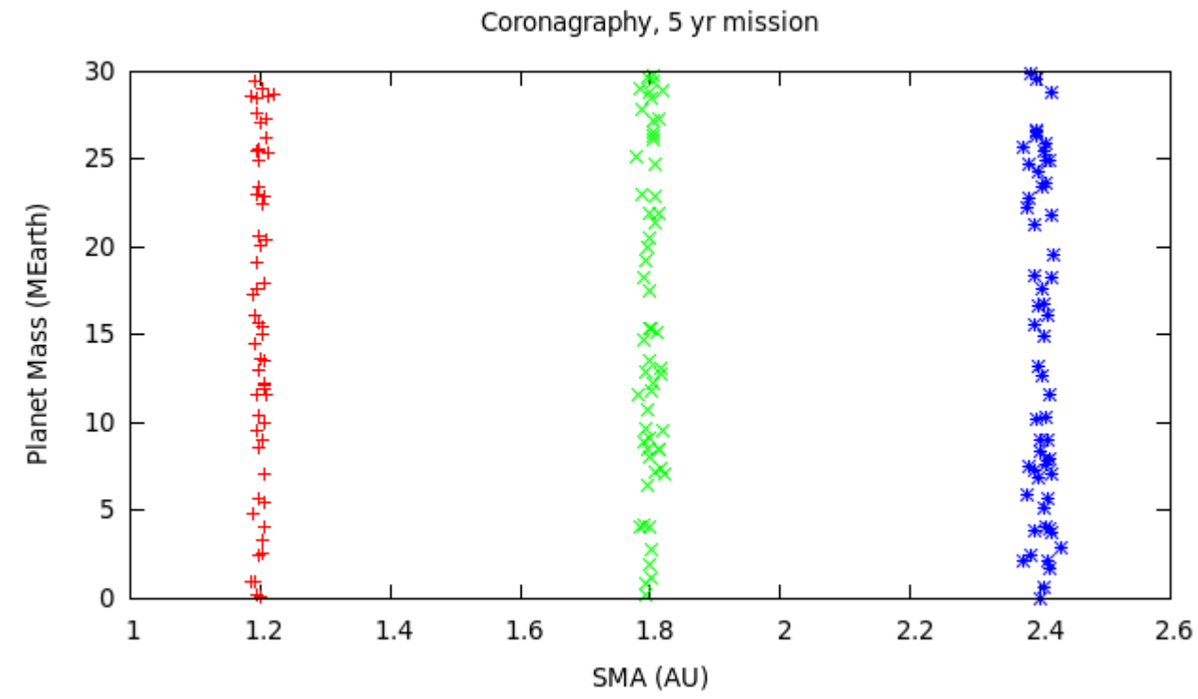

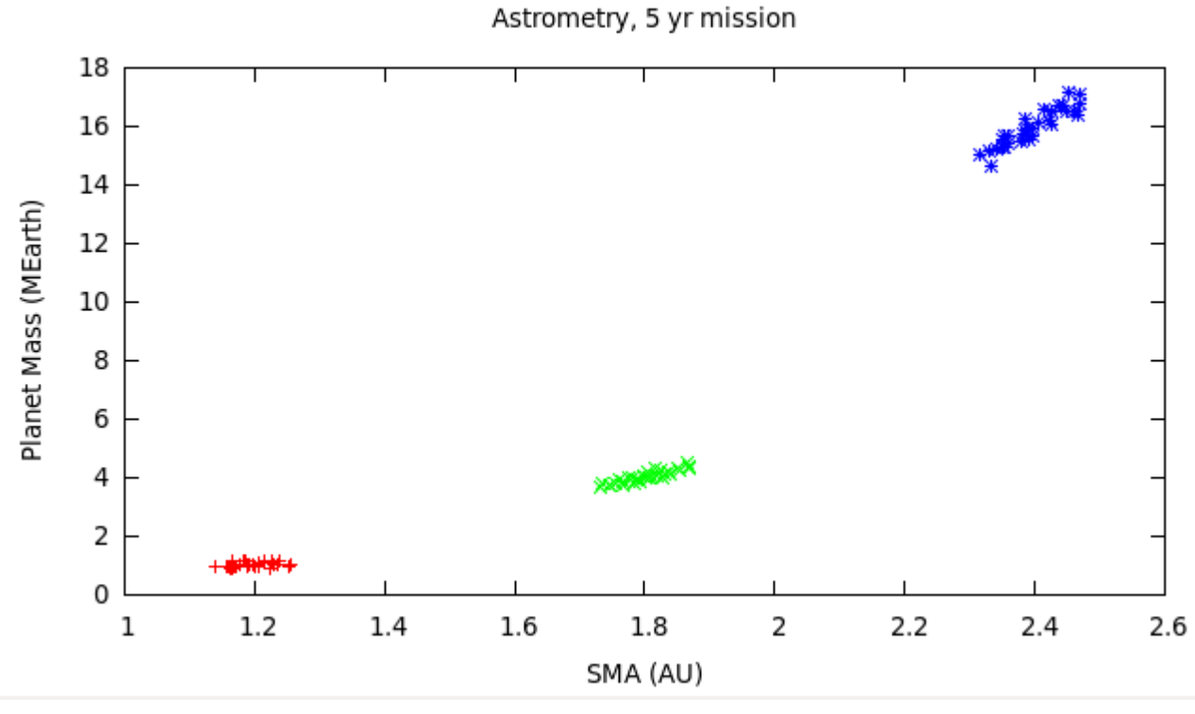

Mass can be constrained quickly
→ firm identification of Earth-like planets within 1 to 2 yrs

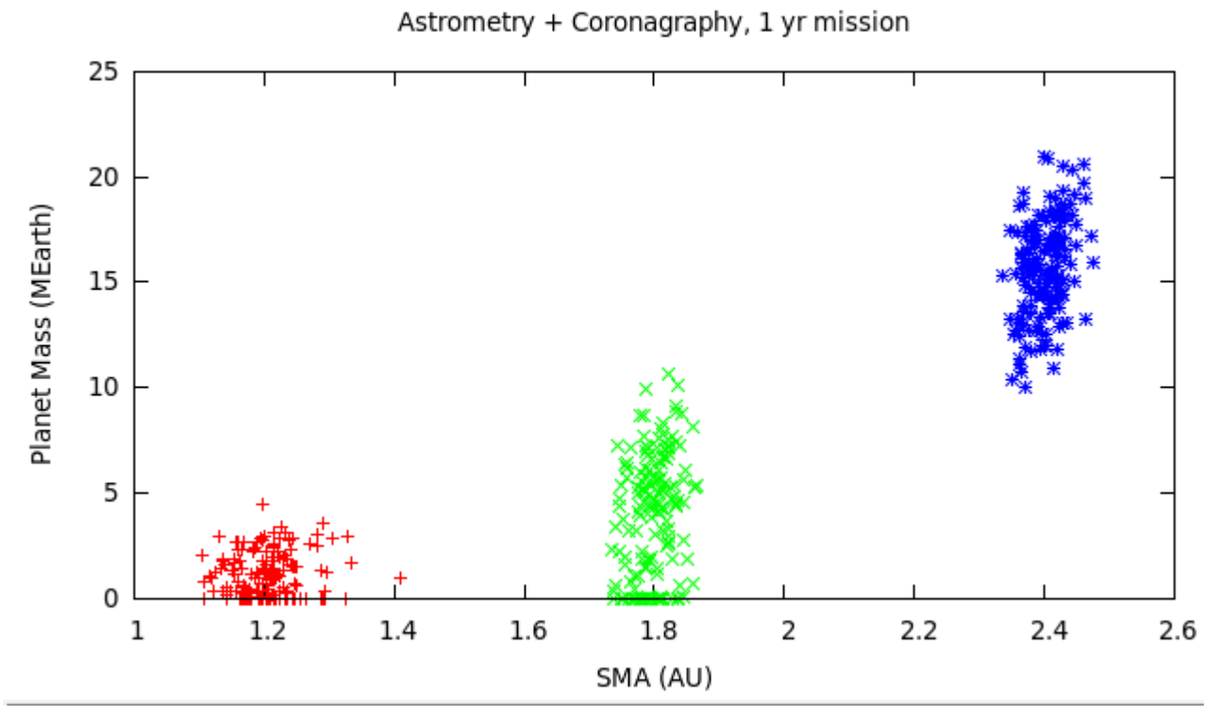

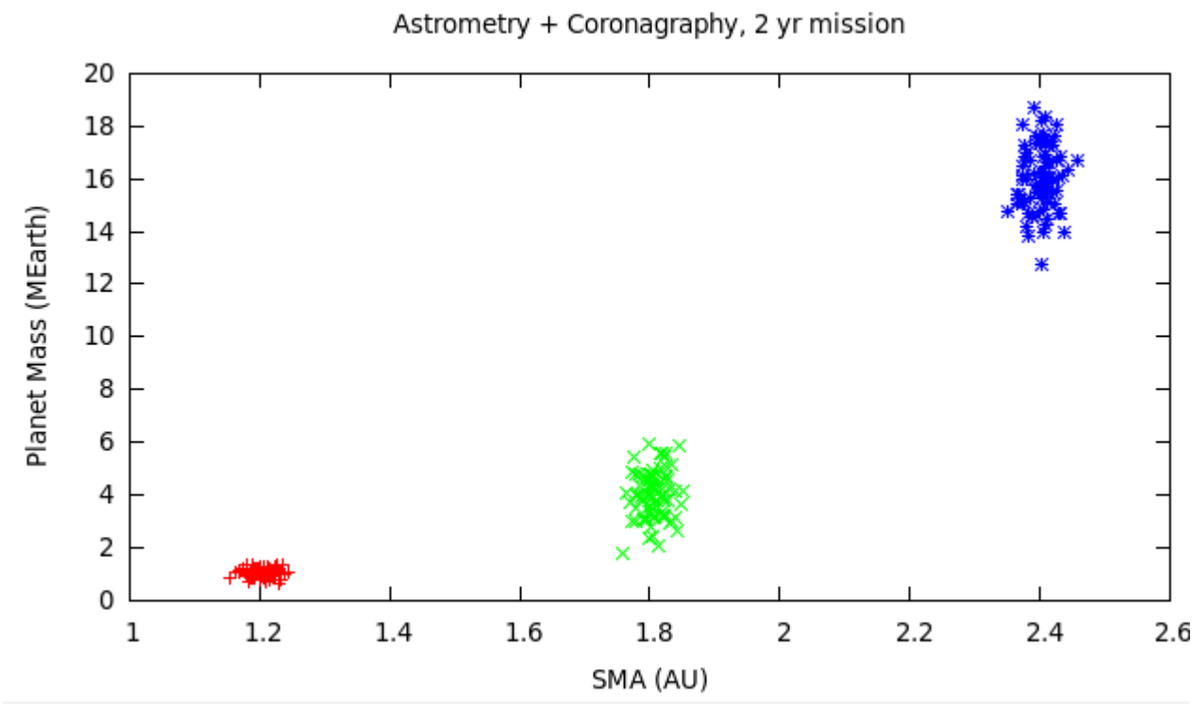

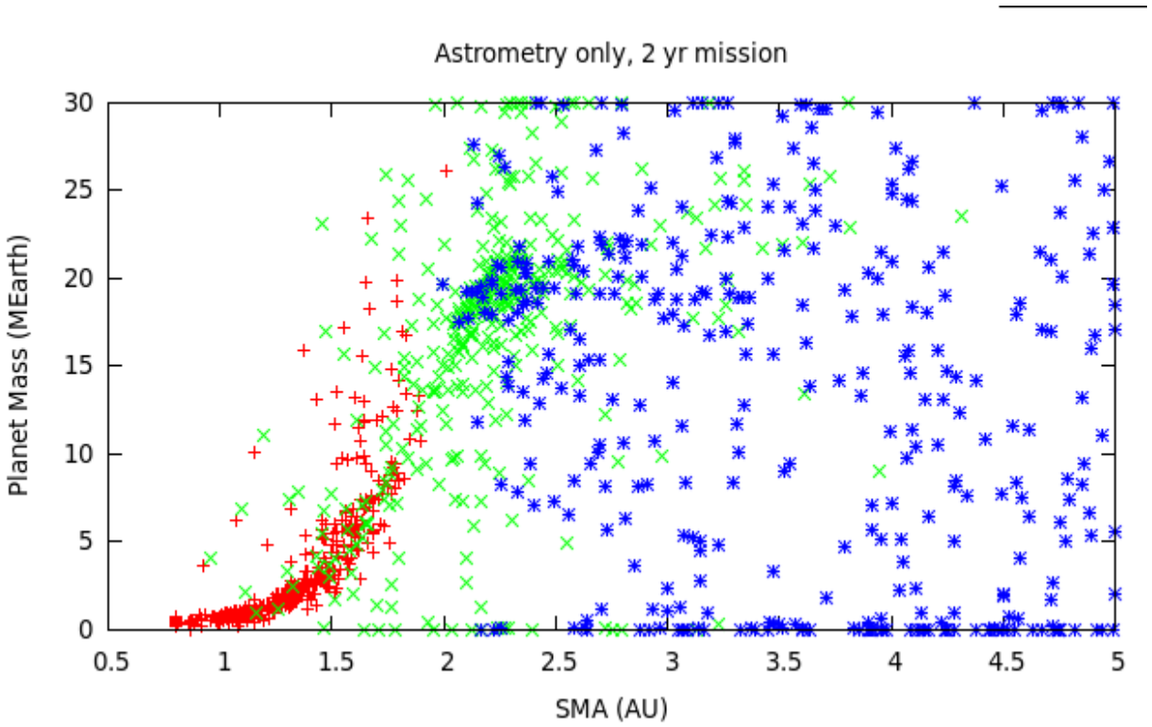
Astrometry only, 2 yr mission
Planet Mass (MEarth)
SMA (AU)
0
5
10
15
20
25
30
0.5
1
1.5
2
2.5
3
3.5
4
4.5
5

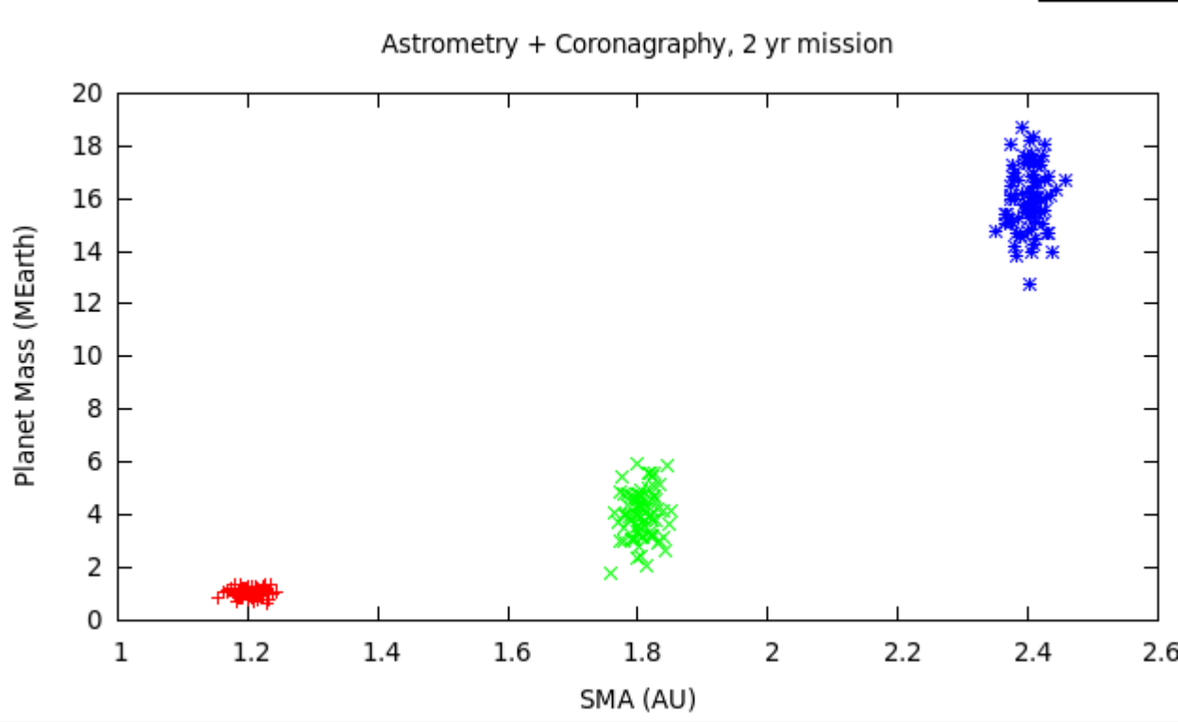
Astrometry + Coronagraphy, 2 yr mission
Planet Mass (MEarth)
SMA (AU)
0
2
4
6
8
10
12
14
16
18
20
1
1.2
1.4
1.6
1.8
2
2.2
2.4
2.6

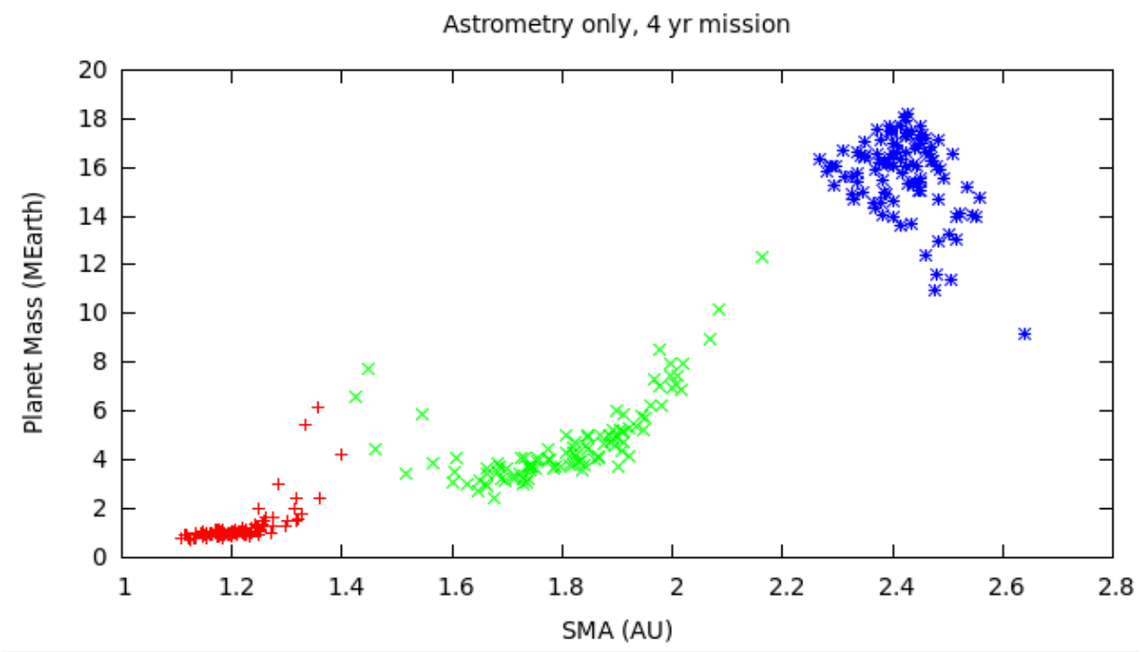
Astrometry only, 4 yr mission
Planet Mass (MEarth)
SMA (AU)
0
2
4
6
8
10
12
14
16
18
20
1
1.2
1.4
1.6
1.8
2
2.2
2.4
2.6
2.8

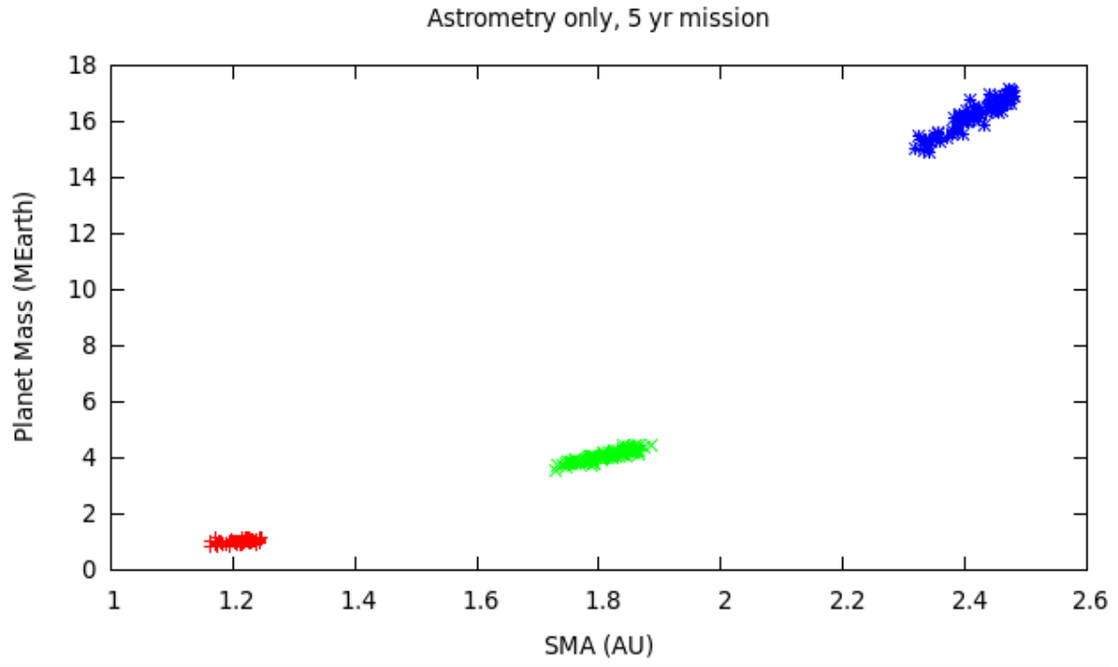
Astrometry only, 5 yr mission
Planet Mass (MEarth)
SMA (AU)
0
2
4
6
8
10
12
14
16
18
1
1.2
1.4
1.6
1.8
2
2.2
2.4
2.6

8 % area coverage on PM
m_V = 3.7 target
Galactic pole observation
2 day per observation

Larger telescope diameter :
- more light in spikes (D^2), finer spikes (1/D) → spike calibration accuracy goes as D^{-2}
- more light in background stars (D^2), and smaller PSF (1/D) → position measurement goes as D^{-2}

Astrometric accuracy goes as D^{-2} $FOV^{-0.5}$
Number of pixels goes as D^{-2} FOV
At fixed number of pixels, larger D is better

But: mean surface brightness of spikes gets fainter as FOV increases

	FOV = 0.03 sq deg	**FOV = 0.1 sq deg**	**FOV = 0.25 sq deg**	**FOV = 0.5 sq deg**	**FOV = 1.0 sq deg**
D = 1.4 m	0.58 *μ*as	0.31 *μ*as	0.20 *μ*as	0.14 *μ*as	0.11 *μ*as
D = 2.0 m	0.28 *μ*as	0.15 *μ*as	0.10 *μ*as	0.07 *μ*as	0.05 *μ*as
D = 3.0 m	0.13 *μ*as	0.067 *μ*as	0.044 *μ*as	0.030 *μ*as	0.024 *μ*as
D = 4.0 m	0.071 *μ*as	0.038 *μ*as	0.025 *μ*as	0.017 *μ*as	0.013 *μ*as

D = 4.0m, FOV = 0.1 sq deg → 0.2 uas in <2hr

Lab testbed at U of Arizona
(work by PhD student E. Bendek)

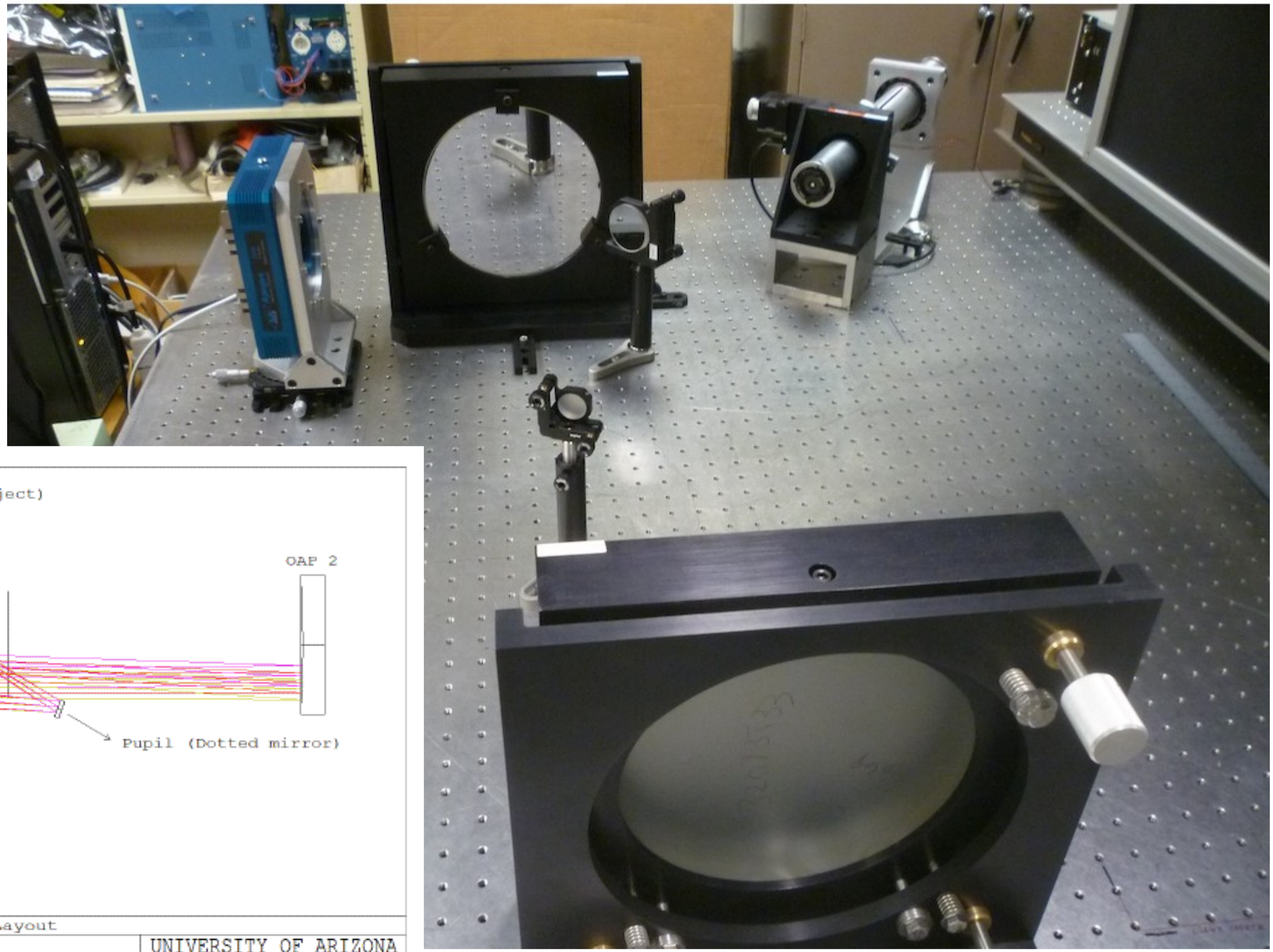

3D Layout

8/14/2011

UNIVERSITY OF ARIZONA
STEWARD OBSERVATORY
ASTROMETRY TEST BED OPTICAL DESIGN

Configuration 1 of 1

Light source design
(work by PhD student E. Bendek)

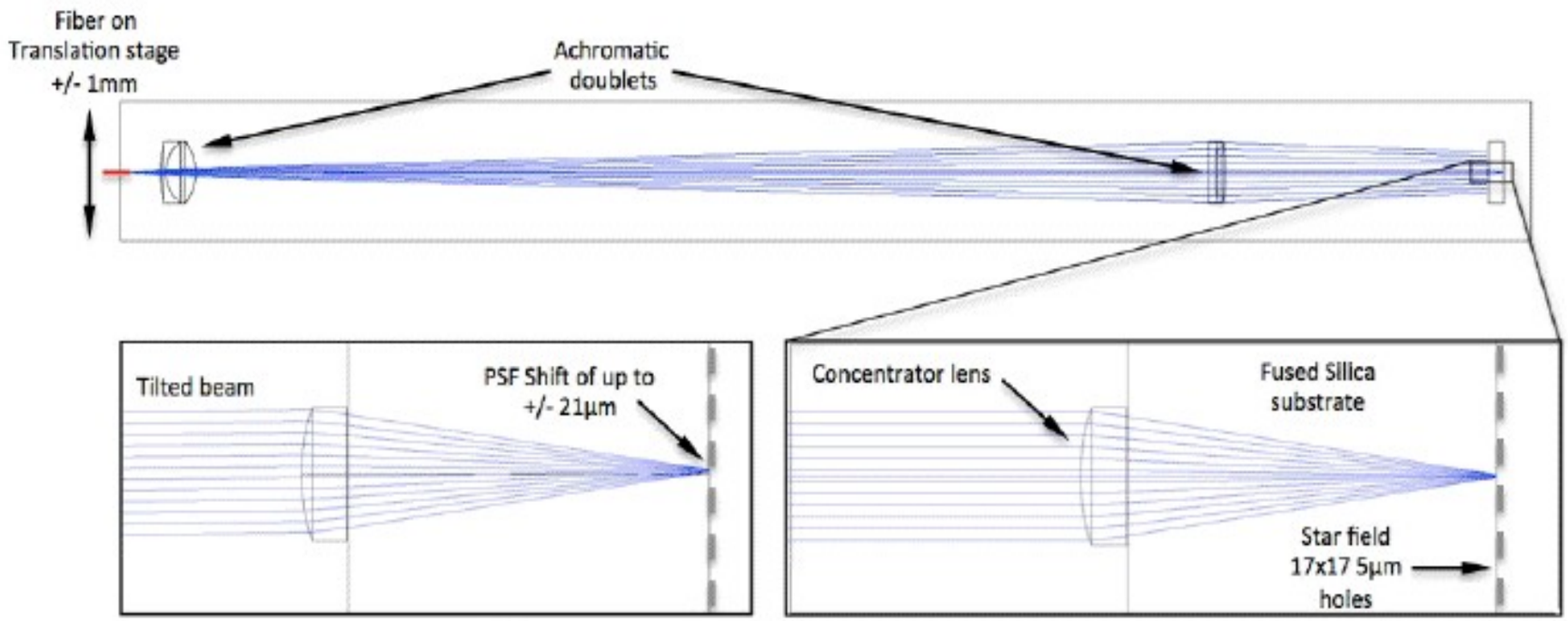

Figure 5. ZEMAX model of the light source, the star simulator substrate and the concentrator lens that increases the brightness of the central star by a factor of $1.5x10^4$ but conserves the diffraction angle by having the same hole size in the coating. The lower image on the left shows how the astrometric signal is generated. In this case, a 1mm displacement of the fiber source translates into 24µm motion of the central star PSF.

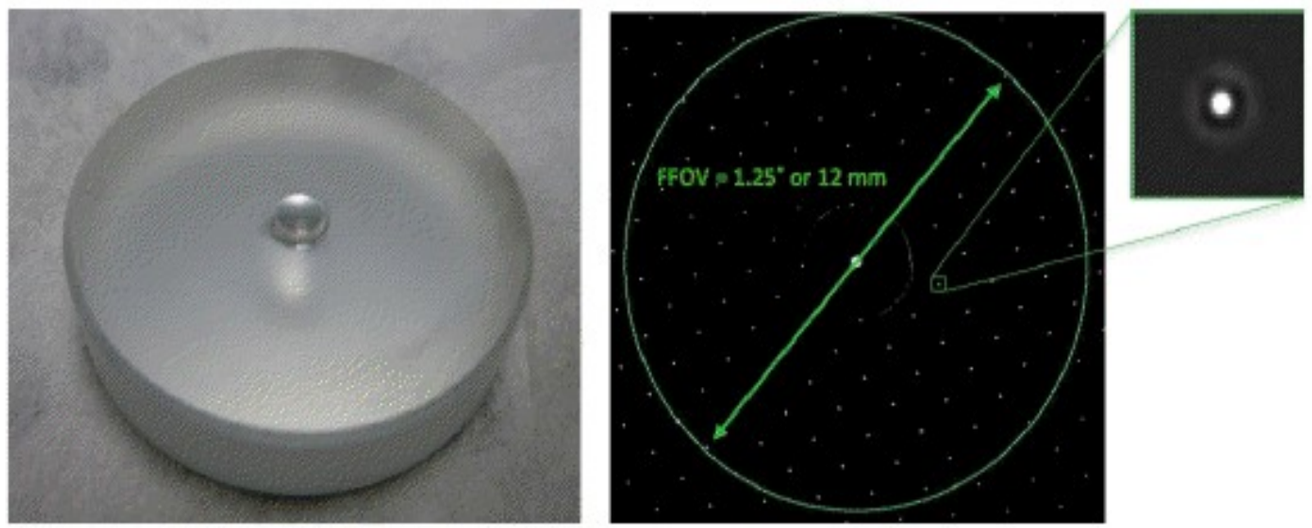

Figure 6. The image on the left shows the substrate with the concentrator lens glued in the back. The image on the right shows the simulated star field

Lab demonstration: early results (work by PhD student E. Bendek)

Diffraction spikes have been imaged in lab
Distortions are measured by spikes displacement

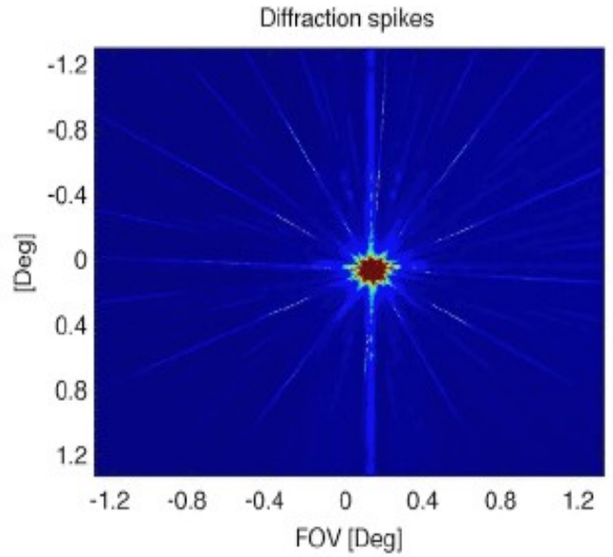

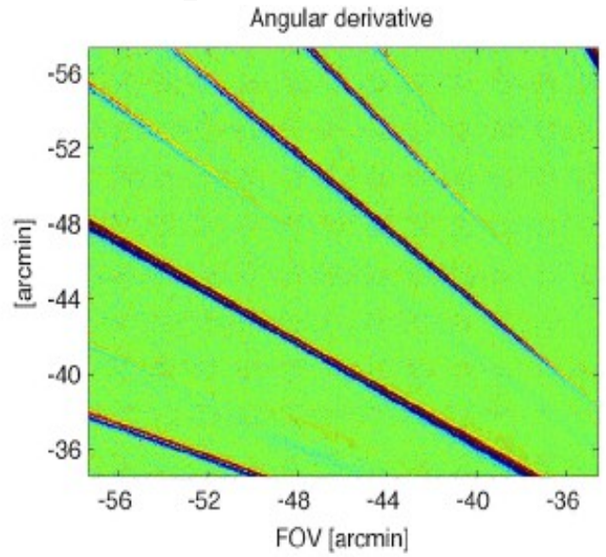

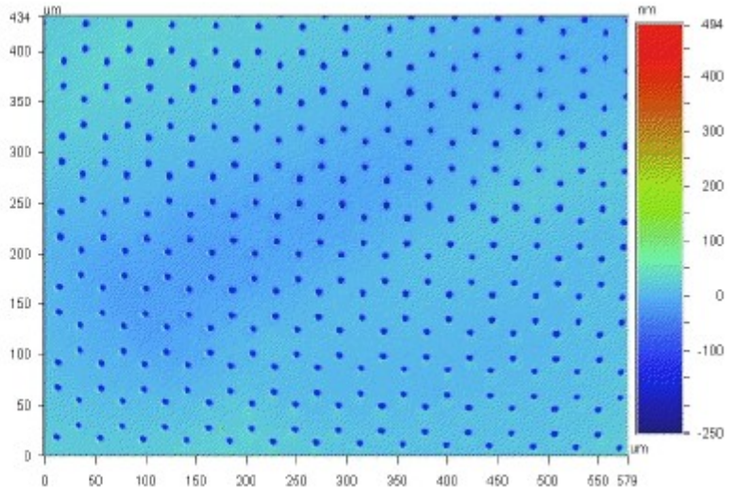

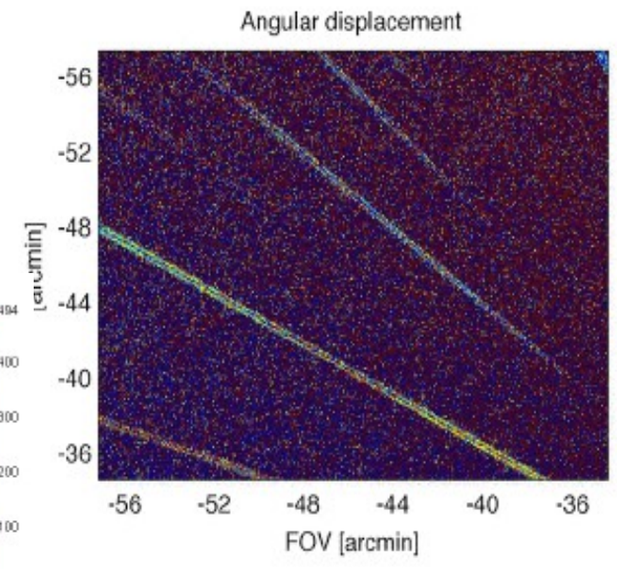

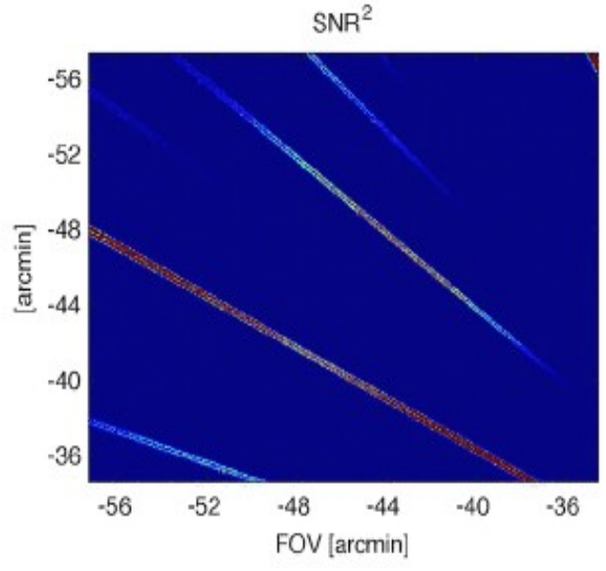

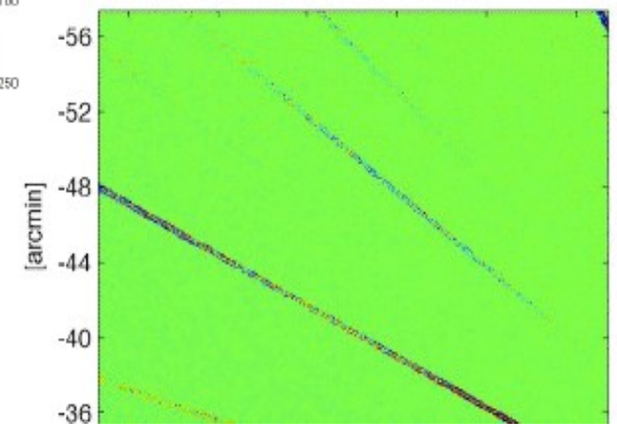

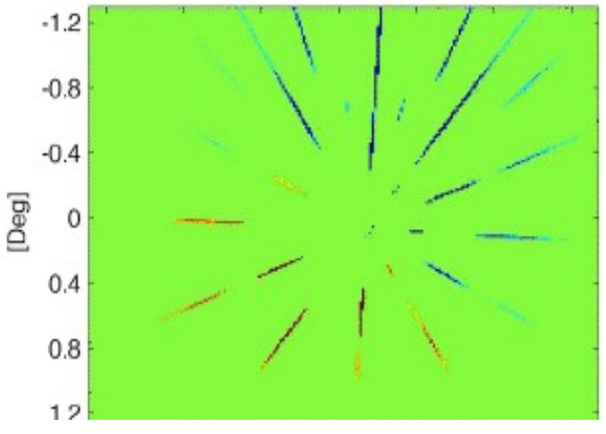

Conclusions

For more info:
http://www.naoj.org/staff/guyon/04research.web/30astrometry.web/content.html

Wide field imaging, coronagraphy and astrometry could be done on the same telescope, simultaneously, without impacting each other
→ should be studied for next generation space optical/UV telescope

Simultaneous astrometry + coronagraphy is extremely powerful
- Improved detection
- Mass measurement

On-sky demonstration and science considered

Lab demo has started at U of Arizona will be used to validate error budget and data reduction

Tests on coronagraphs (Ames, JPL) under preparation